Bull. ERS, No. 21 (1988)

STRONG-MOTION RECORDS OF THE CHIBAKEN-TOHO-OKI EARTHQUAKE OF DECEMBER 17, 1987

Tsuneo KATAYAMA (I)
and
Nobuhiko SATO (II)

SUMMARY

This paper briefly summarizes the characteristics of the Chibaken-Toho-Oki earthquake of December 17, 1987, recorded at the Chiba Experiment Station of the Institute of Industrial Science, University of Tokyo. The array of 36 surface and inground seismometers successfully recorded the ground motion, whose peak acceleration reached as large as 398 cm/s/s. In spite of the large acceleration level, the spectrum intensity (SI) defined as the average amplitude of the 20%-damped velocity response spectrum in the range of 0.1 to 2.5 s was approximately 15 cm/s near the surface of the ground. This level was about one half of the SI needed to cause substantial damage to structures in general.

THE EARTHQUAKE

The Chibaken-Toho-Oki earthquake, which means an earthquake that occurred off (=Oki) the east coast (=Toho) of Chiba Prefecture (=Chibaken), shook Chiba Prefecture and the eastern portion of the Metropolitan Tokyo at 11:08 am on December 17, 1978. This magnitude 6.7 earthquake had its epicenter at 140° 29'E and 35° 21'N with a focal depth of 58 km. Figure 1 shows the location of the epicenter and the distribution of ground motion severity as expressed by the Japan Meteorological Agency's intensity scale [1].

The earthquake caused 2 deaths in Chiba Prefecture. As of December 23, 1987, twelve persons were reported severly injured, seven in Chiba Prefecture and five in Tokyo, and there were a total of 60 persons with minor injury. The reported number of injured persons increased to 135 as

(I) Professor, Institute of Industrial Science, University of Tokyo
(II) Research Assistant, ditto

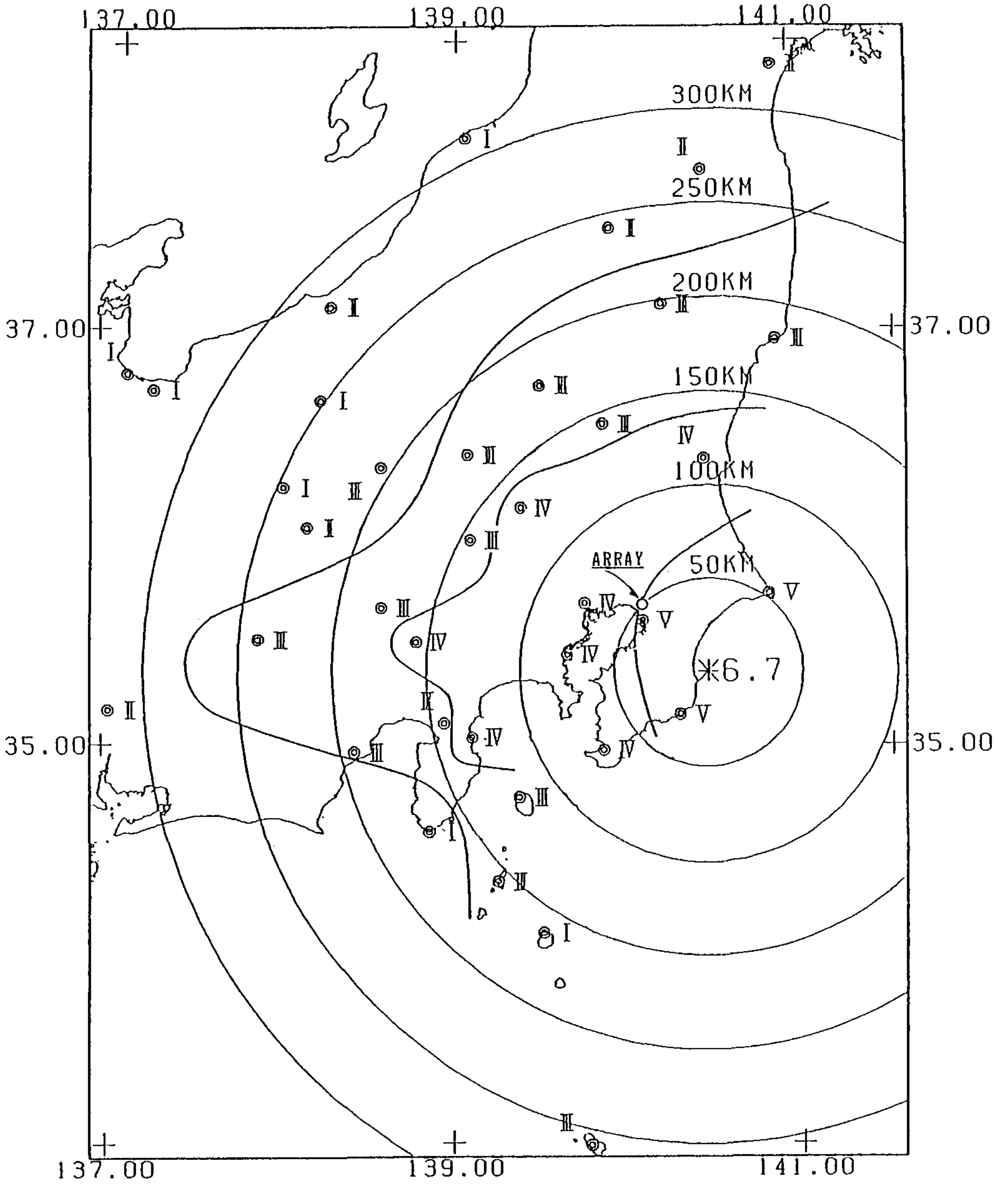

Fig.1 Epicenter and JMA Intensity Distribution [1]

of December 28, 1987.

According to a number of accelerograms obtained in Tokyo and Chiba, the peak acceleration was 400 cm/s/s or even greater in Chiba and it varied between 50 and 150 cm/s/s in Tokyo. In spite of the large peak accelerations recorded, damage to structures and utility systems was minor to moderate although it was widespread with respect to some modes of damage. For example, the number of slightly damaged houses has been reported to be more than 62,000. Liquefaction was also observed at many locations but none of them was damaging to engineered structures. The damage to river, highway (including bridges), sewerage and other public structures under the jurisdiction of the Ministry of Construction amounted to some 2.8 billion yen.

THE ARRAY

The location of the Chiba Experiment Station of the Institute of Industrial Science, University of Tokyo, is shown in Fig.1. The epicentral and hypocentral distances of the site were 46 km and 74 km, respectively. The seismometer array is shown in Fig.2. Although there are four additional boreholes surrounding the array shown in Fig.2, the eight seismometers (-1 m and - 20 m in each borehole) had been damaged by lightening and were under repair at the time of the earthquake. The depths of seismometers in respective boreholes are shown in Table 1. A total of 36 seismometers, each with two horizontal and one vertical components, successfully recorded the ground motion.

The specifications of the seismometers and the digital recorders are summarized in Tables 2 and 3, respectively. The general topography of the site is simple and the subsurface structure is almost uniform within the area concerned. Figure 3 illustrates the soil profiles at three typical boreholes.

More detailed descriptions of the array and the site can be found in Refs. [2] through [5].

THE RECORDS

Figure 4 shows the horizontal motions at different depths in Borehole C0. The peak accelerations are 326 cm/s/s and 216 cm/s/s in the

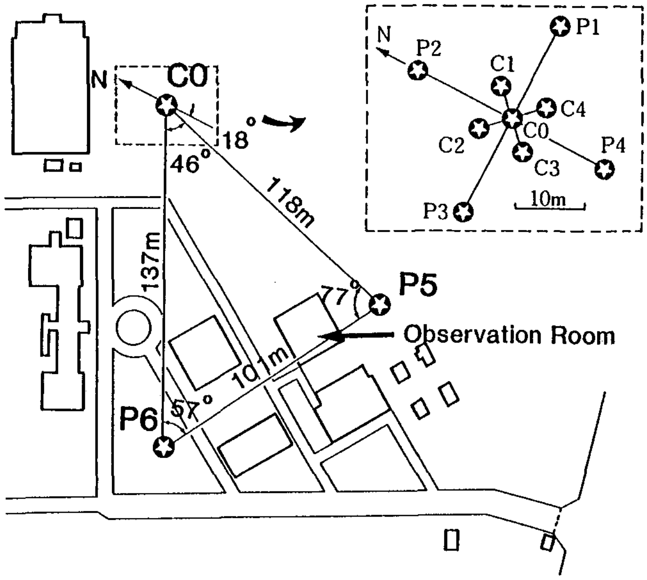

Fig.2 Seismometer Array

Table 1 Depths of Seismometers.

Depth	C0	C1	C2	C3	C4	P1	P2	P3	P4	P5	P6
1m	○	○	○	○	○	○	○	○	○	○	○
5m	○	○	○	○	○						
10m	○	○	○	○	○	○	○	○	○	○	○
20m	○					○	○	○	○	○	○
40m	○									○	

Table 2 Specifications of Borehole Seismometer.

Type of Transducer	: Piezo-electric Accelerometer
Sensing Directions	: 2-Horizontal and Vertical
Full Scale Sensitivity	: 1000 cm/s/s
Sensitivity	: 5 mV for 1 cm/s/s
Frequency Range	: 0.1 to 30 Hz
Output Impedance	: 10
Operating Temperature	: -20 to 40 °C
Transverse Sensitivity	: Max. 3 %
Linearity	: Max. 0.1 % full scale
Water-proofness	: 10 kg/cm/cm
Required Power	: +6 V D-C
Size of Casing	: ϕ 65 x 335 mm
Weight	: 2.5 kg

Table 3 Specifications of Digital Recorder.

Input Channel	: 64 ch.
Input Signal Voltage	: -5 to 5 V
Input Impedance	: 100 k
Input Filter	: Low-pass (0 to 30 Hz)
A/D Converter	: 12 bits
Sampling Rate	: 200 /s
Pre-event Memory	: 1.5 s
Timer Units	: Month, Day, Hour, Minute and Second
Time Correction	: By N.H.K. Radio Broadcast
Seismic Trigger	: Logical Sum or Product of Arbitrary 3 Channels
Trigger Level	: 0.1 to 10 % full scale
Monitoring	: 8 ch. of D/A Converter (12 bits) for Recording or Playback
Recording Medium	: Digital Magnetic Tape (9 tracks, 1600 bpi)
Quake-proofness	: 0.5 g
Dimensions	: 570(w) x 1500(h) x 800(d) mm
Weight	: 75 kg

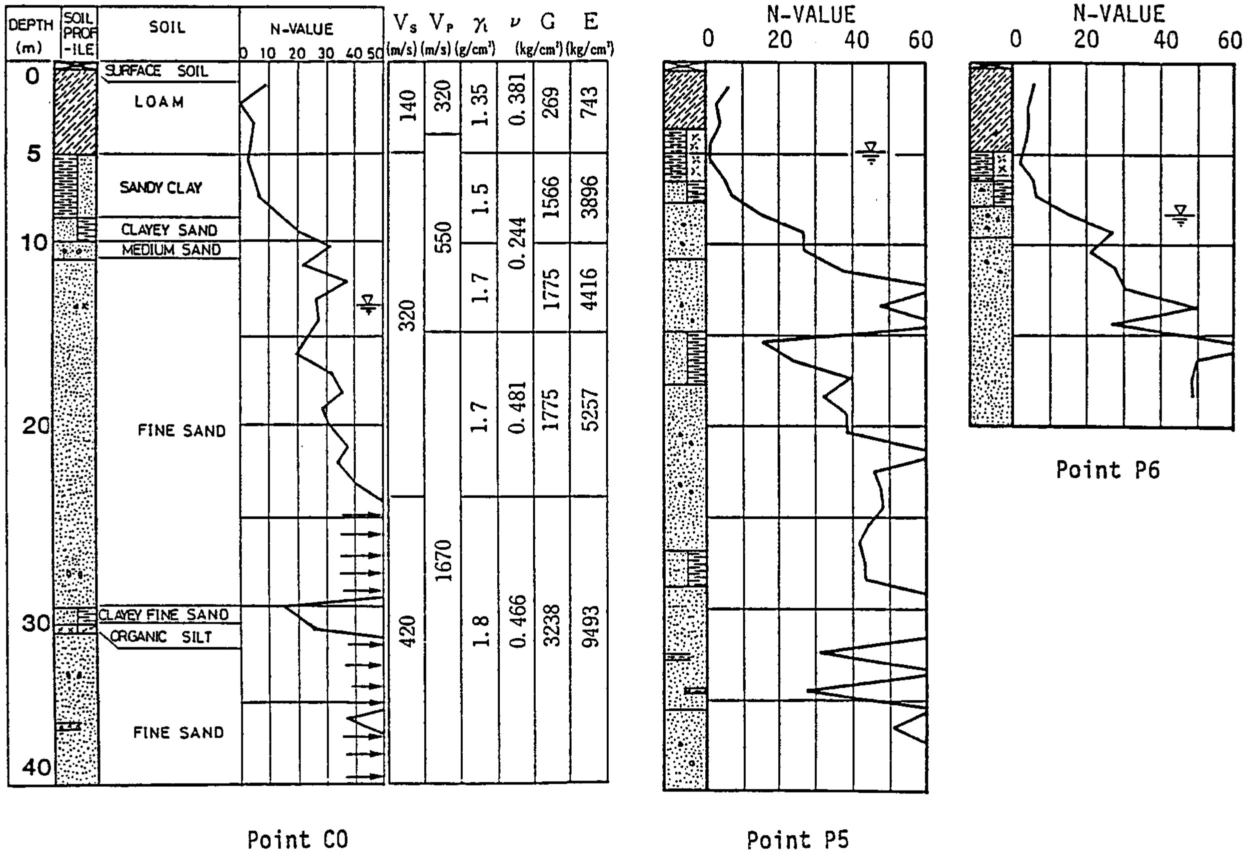

Fig.3 Soil Profiles in Three Typical Boreholes

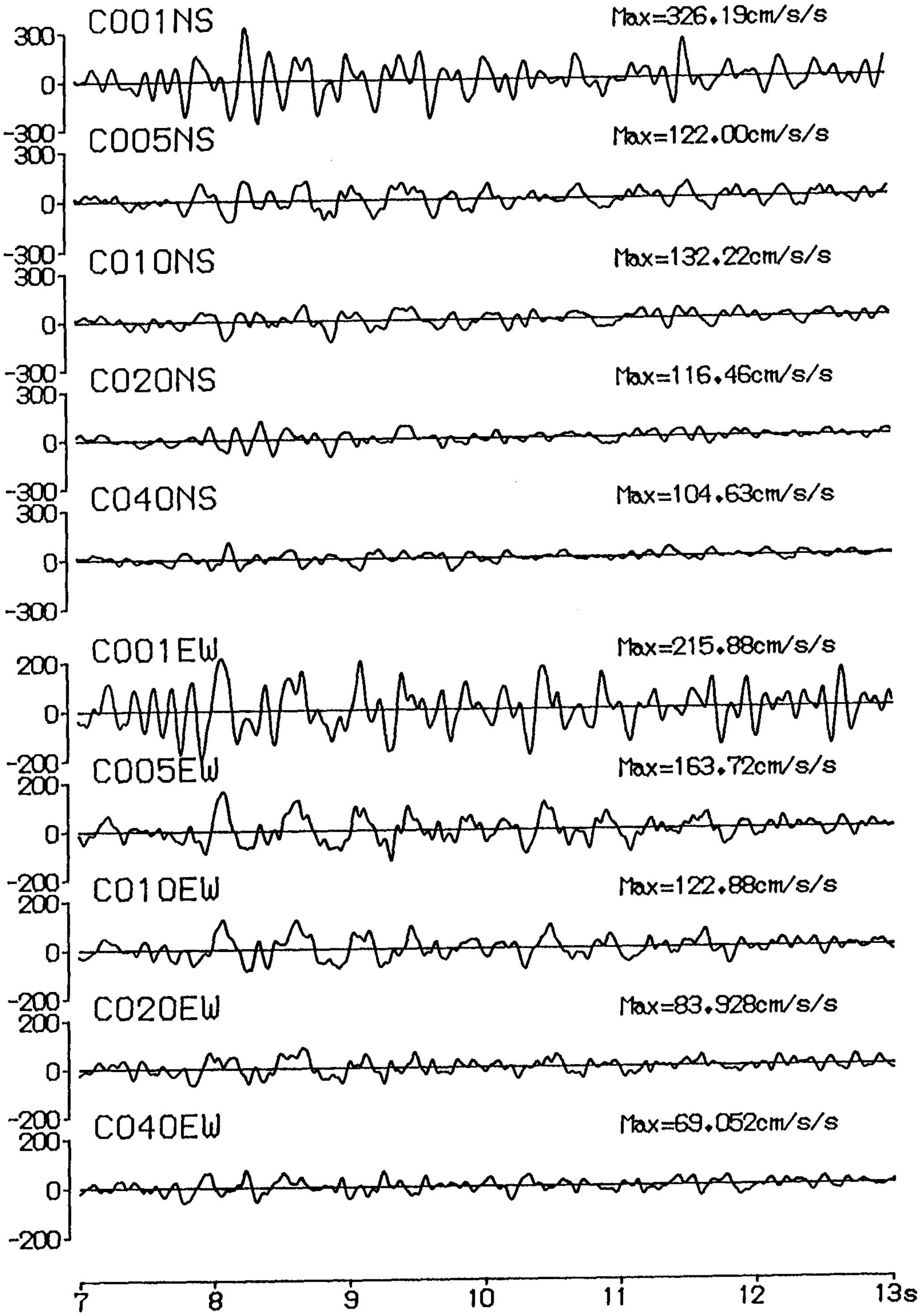

Fig.4 Horizontal Motions at Different Depths in Borehole CO

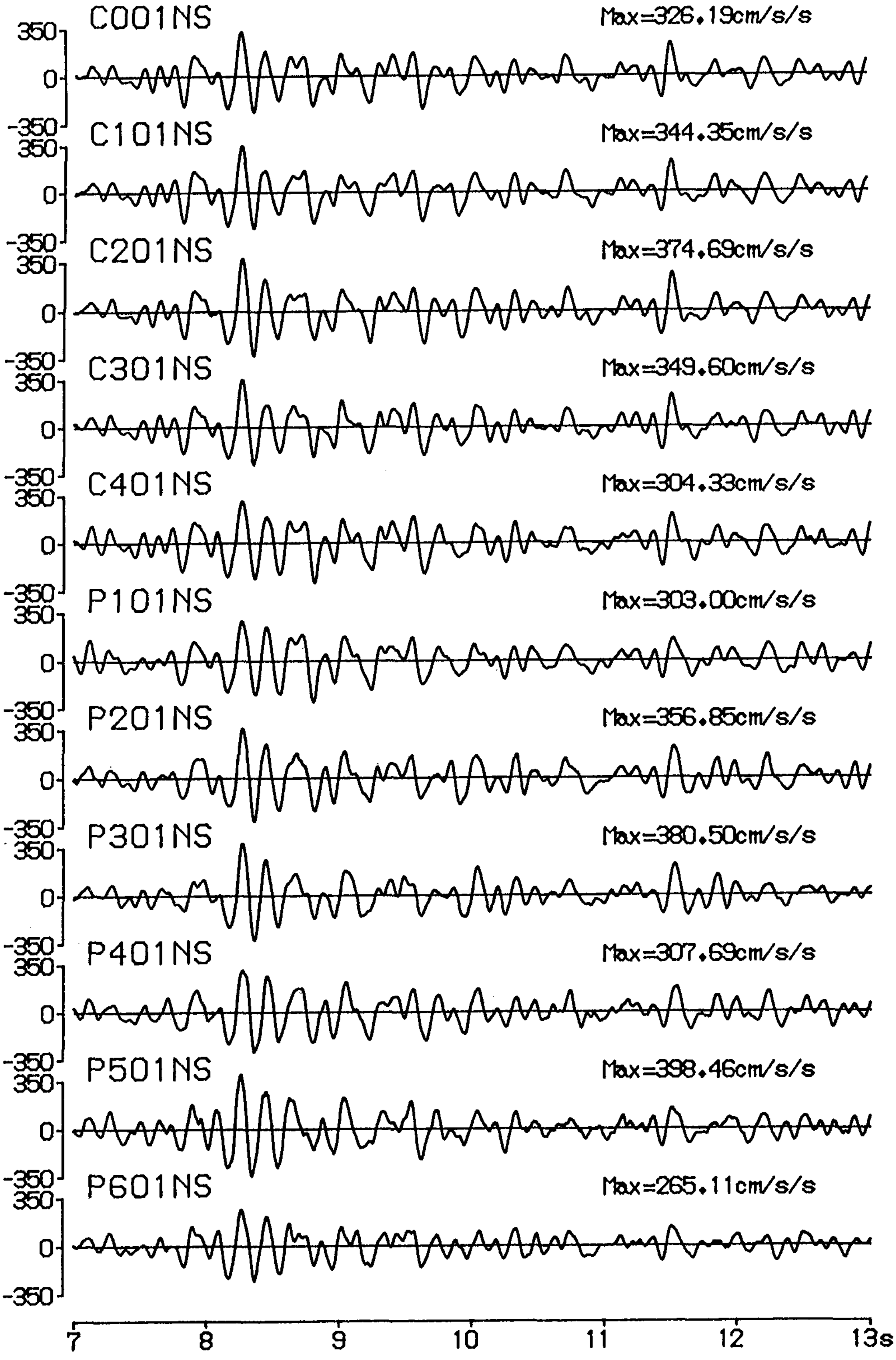

Fig.5 NS-Component Accelerograms at 1m from Ground Surface

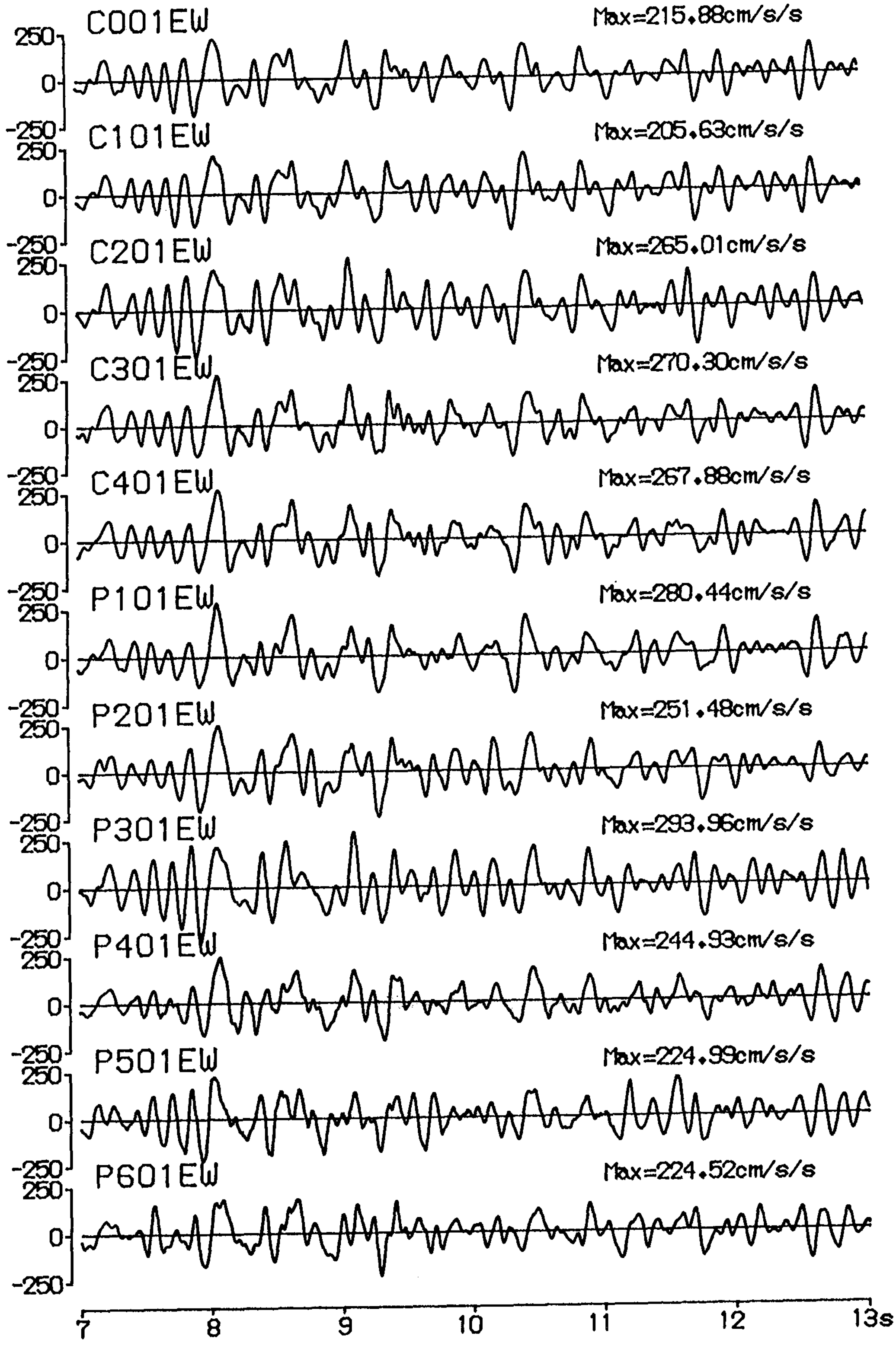

Fig.6 EW-Component Accelerograms at 1m from Ground Surface

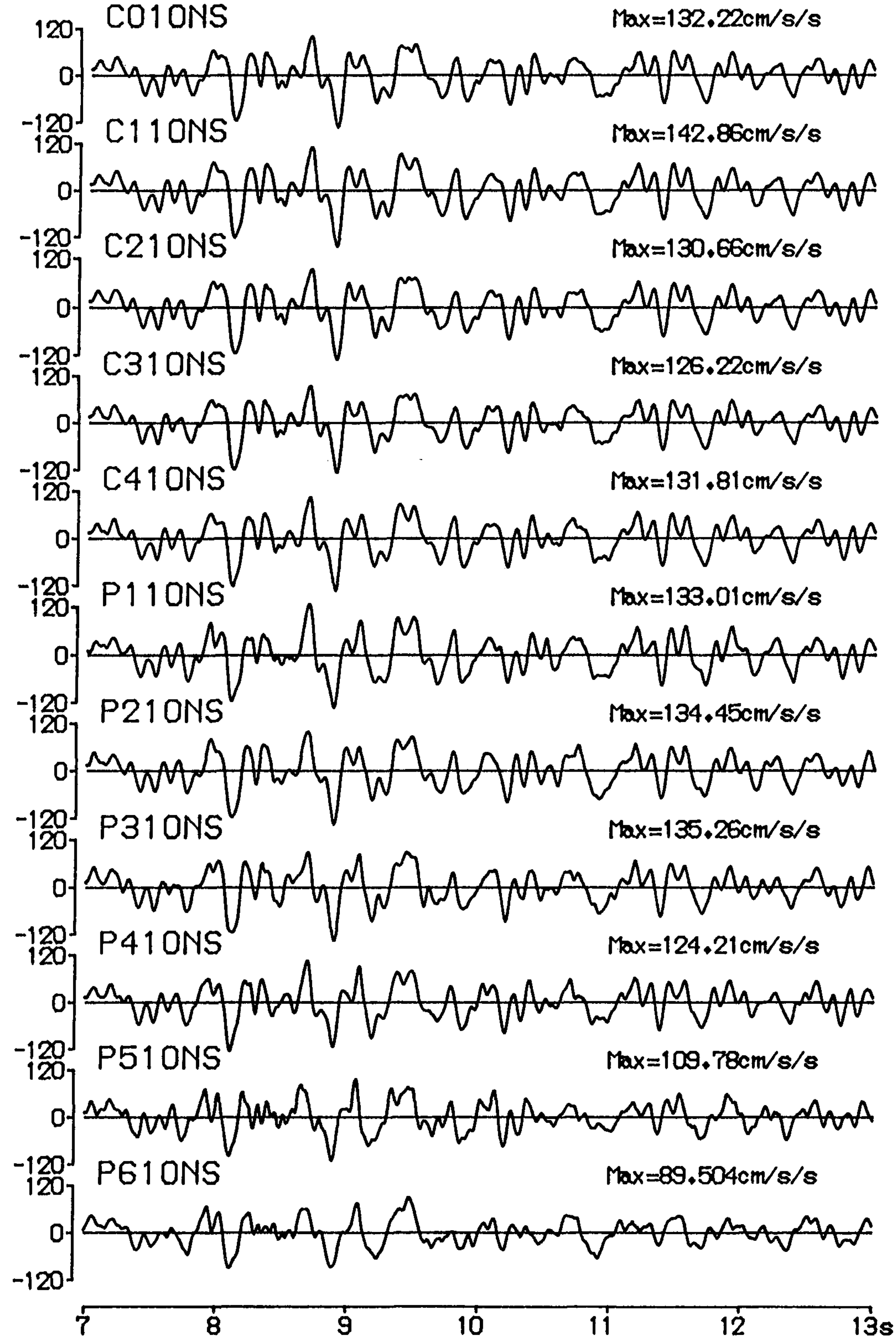

Fig.7 NS-Component Accelerograms at 10m from Ground Surface

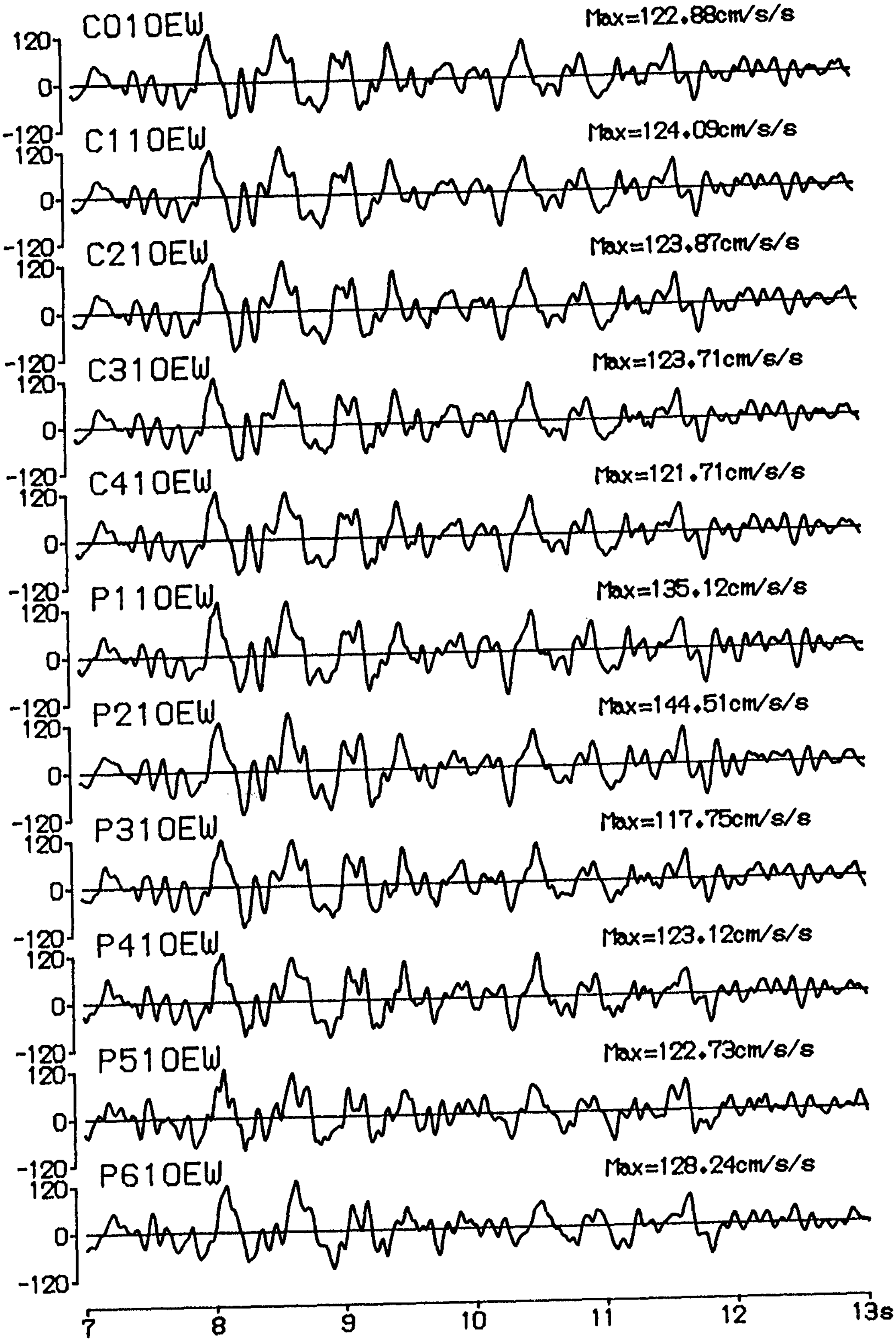

Fig.8 EW-Component Accelerograms at 10m from Ground Surface

north-south and the east-west direction, respectively. The record C001NS, for example, indicates that it is recorded by the north-south component (=NS) of the seismometer at depth 1 m from the ground surface (=01) in Borehole C0.

Eleven horizontal accelerograms recorded at 1 m depth are shown in Fig.5 for the north-south direction and in Fig.6 for the east-west direction. Figures 7 and 8 are similar paste-ups for the accelerograms at 10 m from the ground surface.

Peak accelerations of the three components of the ground motion recorded by all seismometers are summarized in Table 4. The spectrum intensities computed from the records obtained at depths of 1 m and 10 m are summarized in Table 5. The spectrum intensity (=SI) here is defined as the average spectral amplitude of the 20%-damped velocity spectrum over the period range between 0.1 s and 2.5 s [6]. Note that this definition is different from the original one proposed by G.W. Housner.

The following figures show the recorded accelerogram, the computed Fourier spectrum and the 20%-damped velocity response spectrum for selected ground motions. These figures are arranged as follows:

Fig.9 Ground motions at different depths in Borehole C0
- (a) NS and EW components at 1 m from the ground surface
- (b) NS and EW components at 5 m from the ground surface
- (c) NS and EW components at 10 m from the ground surface
- (d) NS and EW components at 20 m from the ground surface
- (e) NS and EW components at 40 m from the ground surface

Fig 10 Ground motions in Borehole C1
- (a) NS and EW components at 1 m from the ground surface
- (b) NS and EW components at 10 m from the ground surface

Fig.11 Ground motions in Borehole C2
- (a) NS and EW components at 1 m from the ground surface
- (b) NS and EW components at 10 m from the ground surface

Fig.12 Ground motions in Borehole C3
- (a) NS and EW components at 1 m from the ground surface
- (b) NS and EW components at 10 m from the ground surface

Fig.13 Ground motions in Borehole C4
- (a) NS and EW components at 1 m from the ground surface
- (b) NS and EW components at 10 m from the ground surface

Table 4 Maximun Peak Accelerations (cm/s/s)

Depth / Direction		Borehole										
		C0	C1	C2	C3	C4	P1	P2	P3	P4	P5	P6
1m	NS	326	344	375	350	304	303	357	381	308	398	265
	EW	216	206	265	270	268	280	251	294	245	225	225
	UD	122	135	131	136	144	155	147	135	169	124	127
5m	NS	122	123	119	120	126						
	EW	164	154	153	174	174						
	UD	80	79	80	78	94						
10m	NS	132	143	131	126	132	133	134	135	124	110	90
	EW	123	124	124	124	122	135	145	118	123	123	128
	UD	61	58	59	64	67	70	61	63	69	63	56
20m	NS	116					119	140	117	98	90	85
	EW	84					80	77	88	81	82	87
	UD	45					41	47	51	43	50	46
40m	NS	105									101	
	EW	69									98	
	UD	43									36	

Table 5 SI-Values (cm/s)

Depth / Direction		Borehole										
		C0	C1	C2	C3	C4	P1	P2	P3	P4	P5	P6
1m	NS	15	15	15	15	15	16	15	15	16	15	13
	EW	15	15	15	16	16	15	16	15	15	13	14
10m	NS	9	10	9	9	9	10	9	10	9	9	8
	EW	11	11	11	10	11	11	11	11	11	10	11

Fig.14 Ground motions in Borehole P1

(a) NS and EW components at 1 m from the ground surface

(b) NS and EW components at 10 m from the ground surface

Fig.15 Ground motions in Borehole P2

(a) NS and EW components at 1 m from the ground surface

(b) NS and EW components at 10 m from the ground surface

Fig.16 Ground motions in Borehole P3

(a) NS and EW components at 1 m from the ground surface

(b) NS and EW components at 10 m from the ground surface

Fig.17 Ground motions in Borehole P4

(a) NS and EW components at 1 m from the ground surface

(b) NS and EW components at 10 m from the ground surface

Fig.18 Ground motions in Borehole P5

(a) NS and EW components at 1 m from the ground surface

(b) NS and EW components at 10 m from the ground surface

Fig.19 Ground motions in Borehole P6

(a) NS and EW components at 1 m from the ground surface

(b) NS and EW components at 10 m from the ground surface

PRELIMINARY DISCUSSIONS

The means, standard deviations, and the coefficients of variation are summarized in Table 6 for the peak acceleration and the spectrum intensity. Eleven sample values are available for both of them at the depths of 1 m and 10 m from the ground surface. The mean peak acceleration near (i.e. 1 m from) the ground surface is 337 cm/s/s in the north-south direction and 250 cm/s/s in the east-west direction. The general difference in the peak acceleration in these two directions may be easily observed by comparing the accelerograms in Figs. 5 and 6. The coefficient of variation of the peak accelerations within an area with about 100 m radius may be seen to be approximately 10%. This value is generally in good agreement with those obtained for previous earthquakes [7].

Although the difference of the peak accelerations in the two perpendicular directions is significant near the ground surface, it almost disappears at the depth of 10 m. It may be too simple to say that this difference is due to the directivity of the surface layer characteristics, and further analysis is clearly needed.

Table 6 Means, Standard Deviations and Coefficients of Variation of Peak Accelerations (cm/s/s) and Spectrum Intensities (cm/s)

	Depth	NS			EW			UD		
		(1)	(2)	(3)	(1)	(2)	(3)	(1)	(2)	(3)
Peak Acceleration	1 m	337	38	0.11	250	27	0.11	139	14	0.10
	10 m	126	14	0.11	126	7	0.06	63	4	0.07
Spectrum Intensity	1 m	15.0	0.7	0.05	15.0	0.9	0.06	--	--	--
	10 m	9.2	0.6	0.06	10.8	0.4	0.04	--	--	--

(1)Mean

(2) Standard Deviation

(3) Coefficient of Variation

The amplification of acceleration from 10 m to 1 m from the ground surface is approximately 2 to 2.5, which seems to be slightly smaller than those obtained during weaker shakings. However, more detailed analysis is imminent.

It is also interesting to note that the SI values do not show such directional difference even in the ground surface (i.e. -1 m) records. This implies that the damageabilities of the north-south and the east-west ground motion are almost the same in spite of the large apparent difference of the peak accelerations. The spectrum intensity may be a more stable and reliable parameter to describe the effect of seismic ground motion to structures in general.

Finally, the level of SI values should be commented. From the results of the analyses on a number of strong motion records and their associated damage, it has been conclusively found that damage is more strongly related to the spectrum intensity than to the peak acceleration. Based on this finding, the authors tentatively proposed SI=30 cm/s as the threshold to estimate whether or not damage in an area concerned becomes substantial [6]. Although the peak acceleration was definitely in the range of 300 to 400 cm/s/s in the area surrounding the Chiba Experiment Station, damage in the area was negligible because the level of SI was far smaller than the aforementioned threshold. The reasons for SI being small may be attributed to higher dominant frequencies and shorter duration of strong motion phase. Further analysis is also required in this direction.

REFERENCES

[1] Sasaki, Y., "Prompt Report of the Chibaken-Toho-Oki Earthquake of December 17,1987", Doboku Gijutsu Shiryo, 30-1, pp.47-55, Jan., 1987.

[2] Katayama, T., and N. Sato, "Ground Strain Measurements by a Very Densely Located Seismometer Array", Proc. Sixth Japan Earthquake Engineering Symposium, pp.241-248, Dec., 1982.

[3] Katayama, T., J. Farjoodi, and N. Sato, "Measurement of Seismic Ground Strain by a Dense Seismograph Array", Proc. Eighth World Conference on Earthquake Engineering, Vol.II, pp.207-214, July, 1984.

[4] Farjoodi, J., N. Sato, and T. Katayama, "Engineering Properties of Ground Motion Obtained from Dense Seismograph Array Data (Part I: Ground Strain)", Bulletin of ERS, University of Tokyo, No.18, March, 1985.

[5] Sato, N, and T. Katayama, "Ground Motions of October 4 and November 6,1985, Earthquakes Recorded by Dense Seismograph Array", Bulletin of ERS, University of Tokyo, No.19, March, 1986.

[6] Katayama, T., N. Sato, N.Ohbo, M. Kawasaki, and K. Saito, "Ground Shaking Severity Detector by Use of Spectrum Intensity (SI)", Proc. Seventh Japan Earthquake Engineering Symposium, pp.373-378, Dec., 1986.

[7] Katayama, T., and N. Sato, "Scatter of Seismic Ground Properties Determined by Array Observation Records", Preprint, JSCE 39th Annual Meeting, Vol.I, pp.803-804, Oct., 1984.

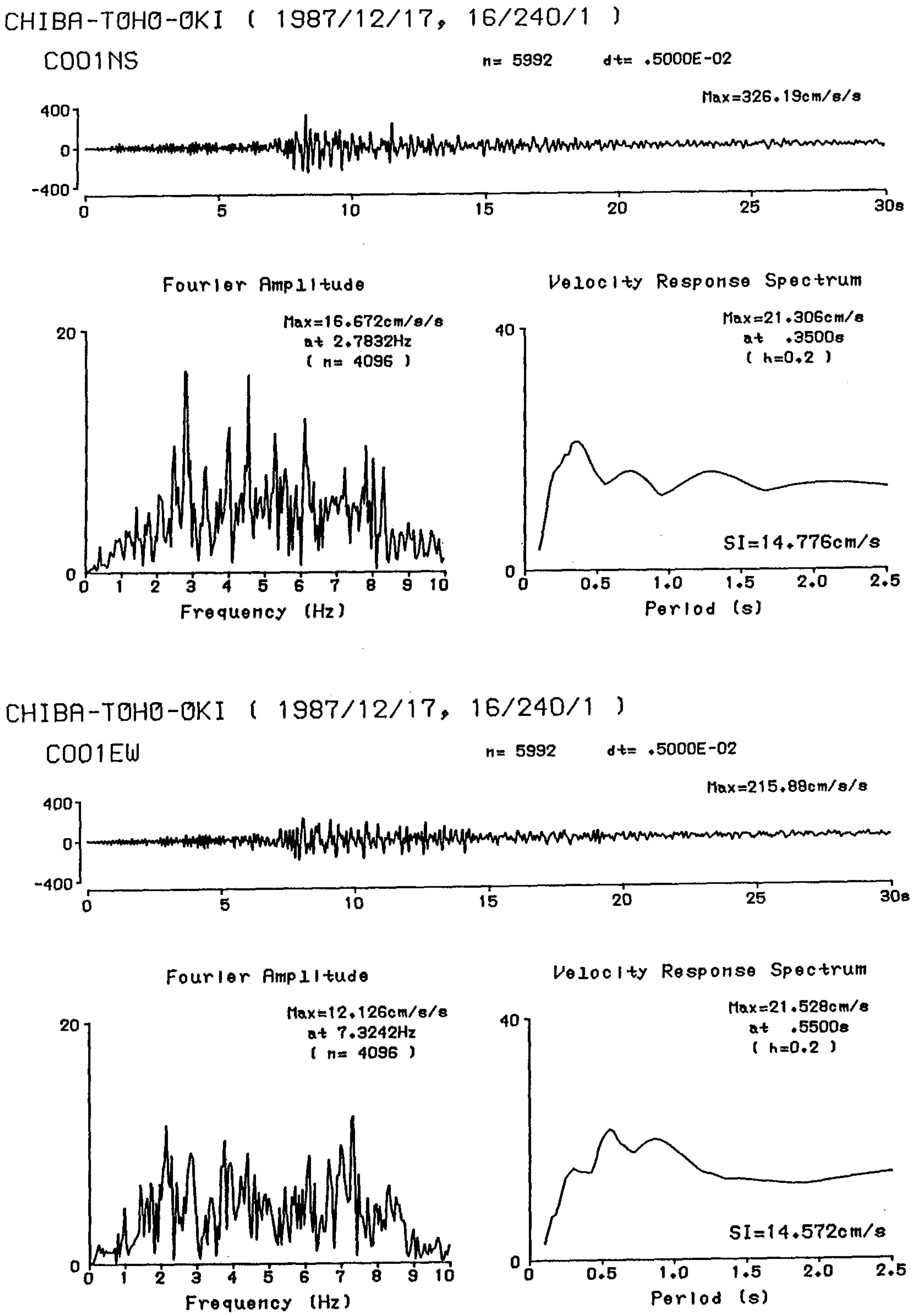

Fig.9(a) Ground Motion at GL-1 in Borehole C0

CHIBA-TOHO-OKI (1987/12/17, 16/240/1)

C005NS

n= 5992 dt= .5000E-02

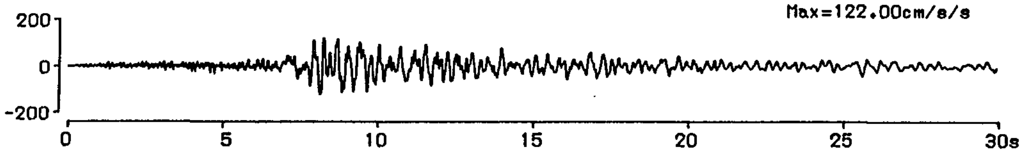

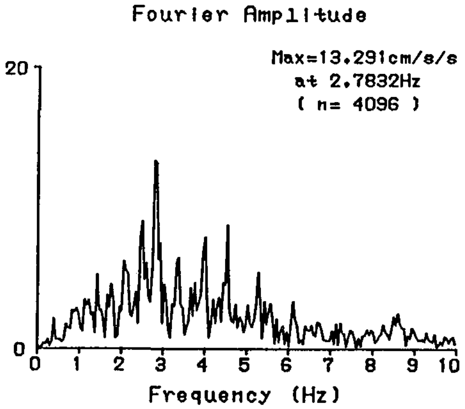

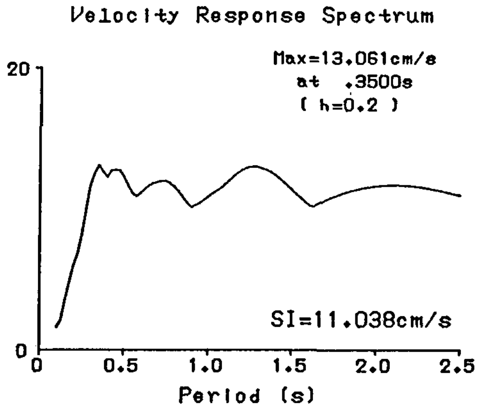

CHIBA-TOHO-OKI (1987/12/17, 16/240/1)

C005EW

n= 5992 dt= .5000E-02

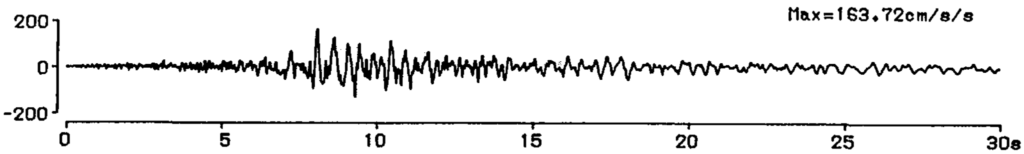

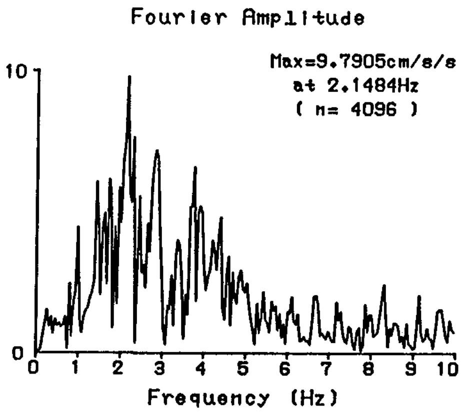

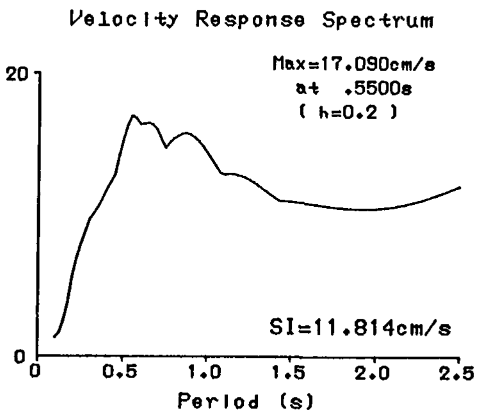

Fig.9(b) Ground Motion at GL-5 in Borehole CO

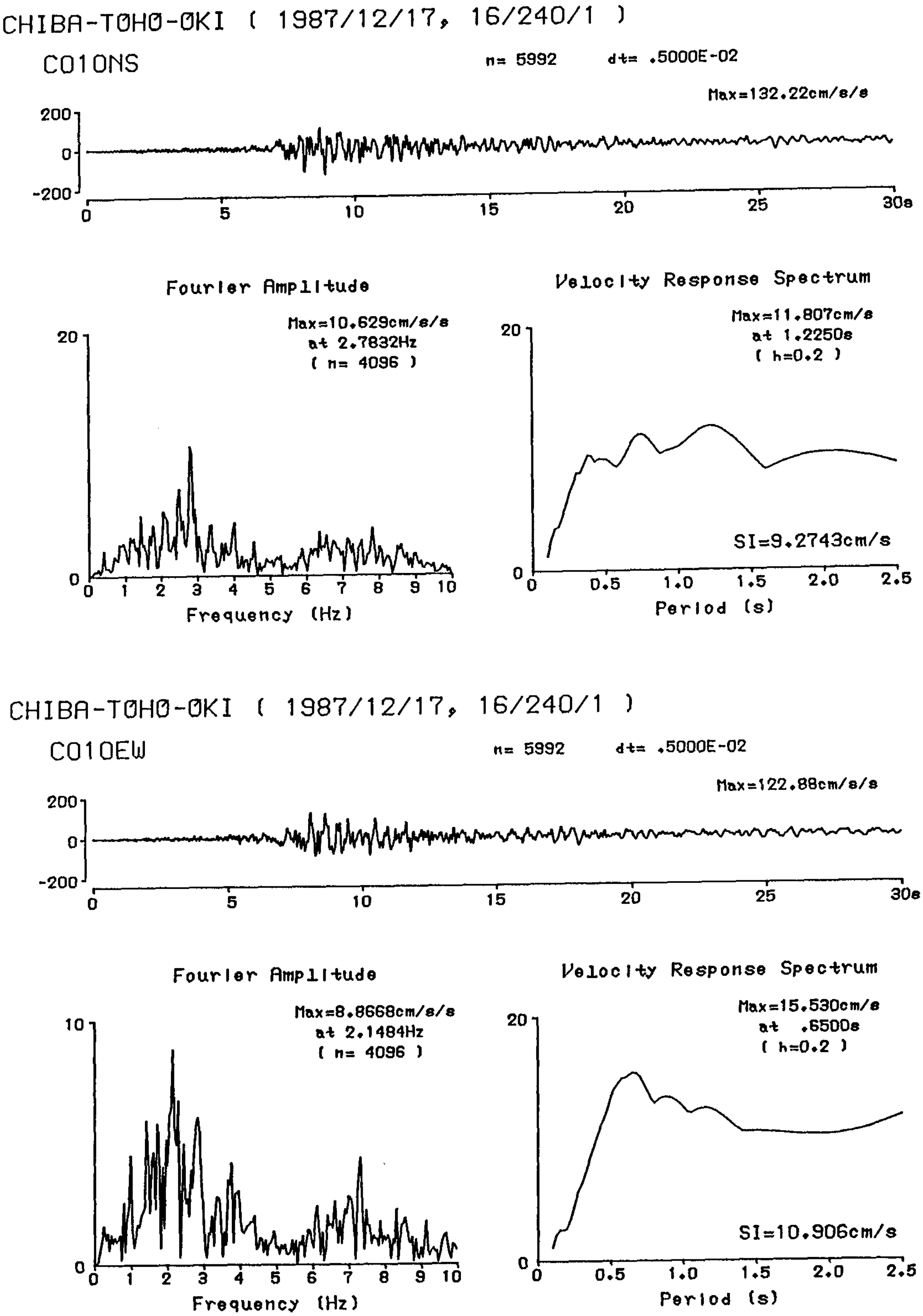

Fig.9(c) Ground Motion at GL-10 in Borehole CO

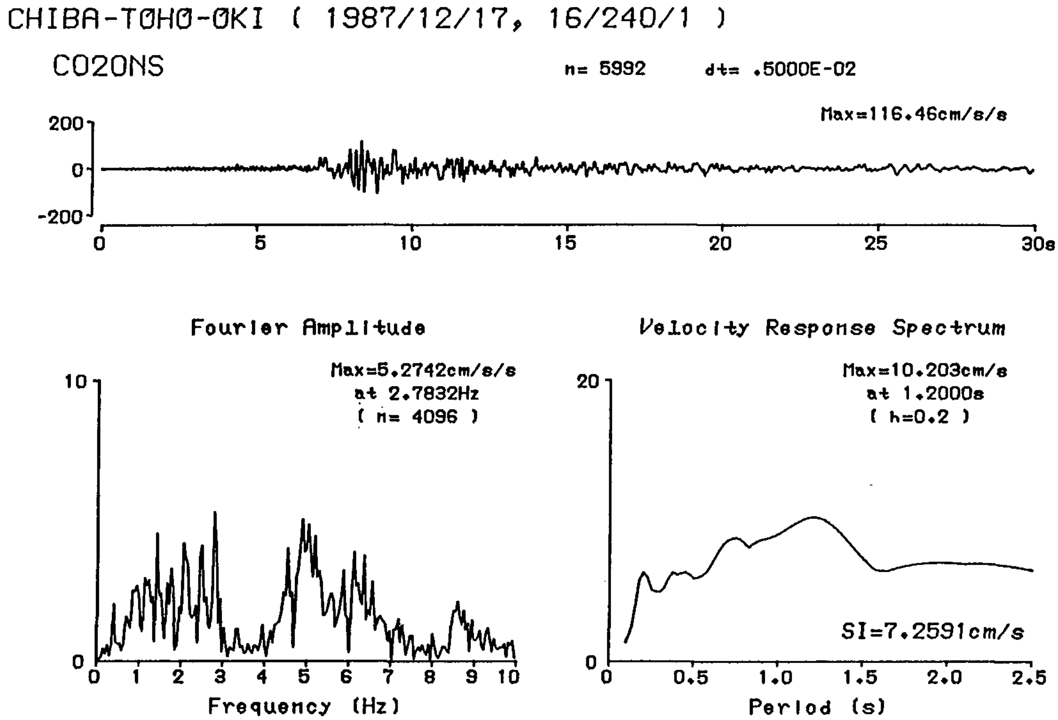

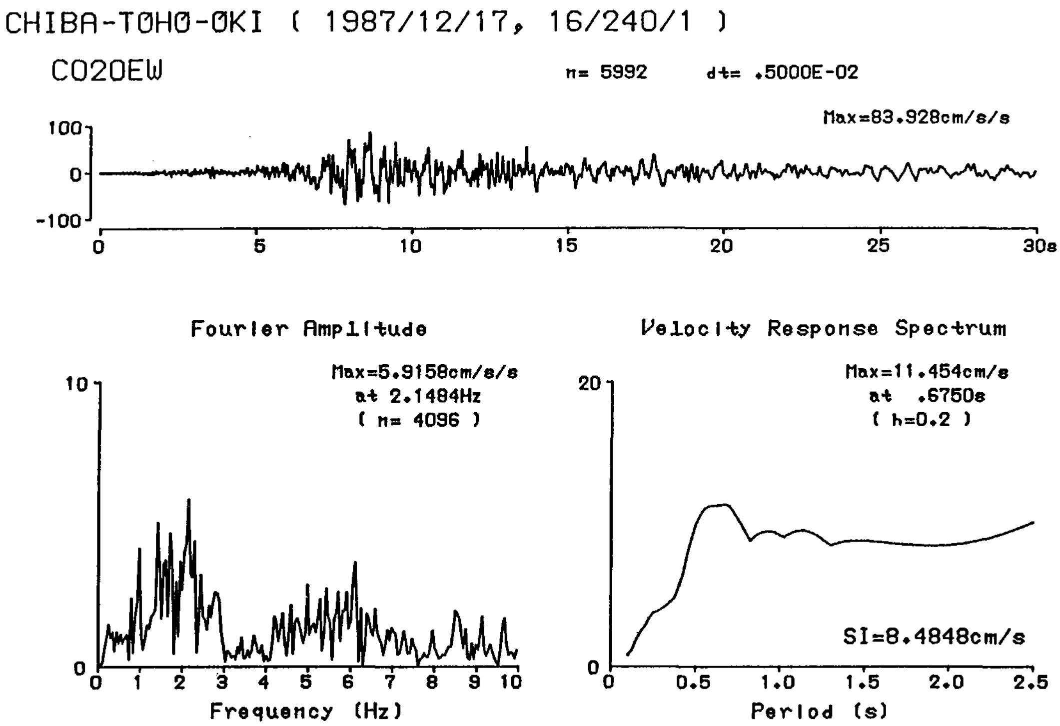

Fig.9(d) Ground Motion at GL-20 in Borehole CO

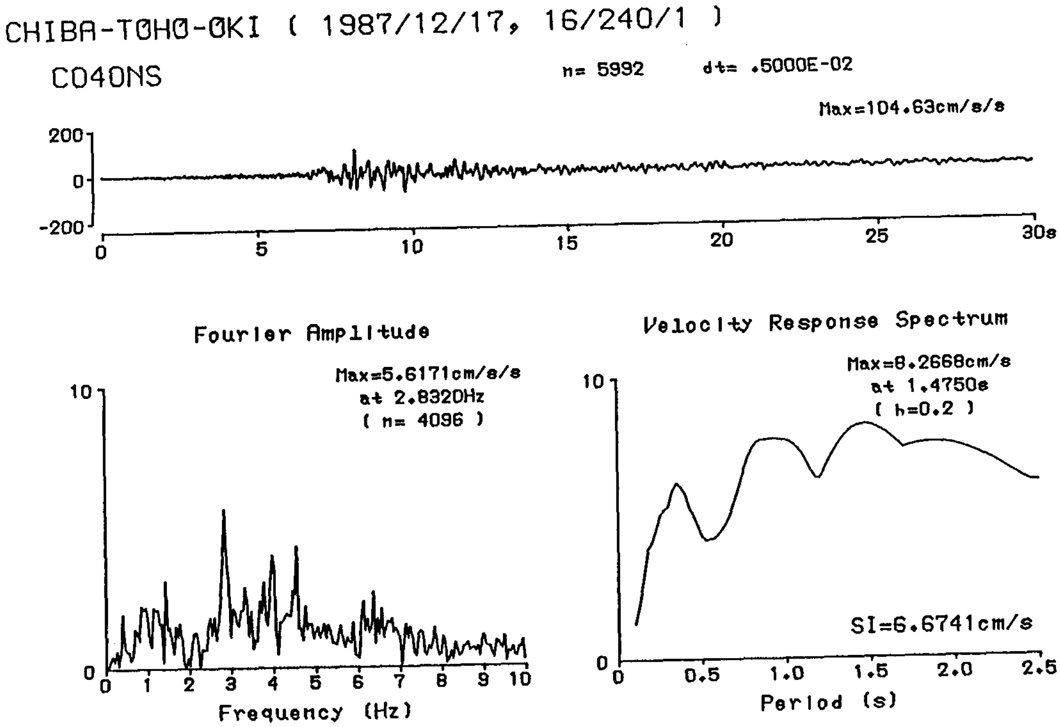

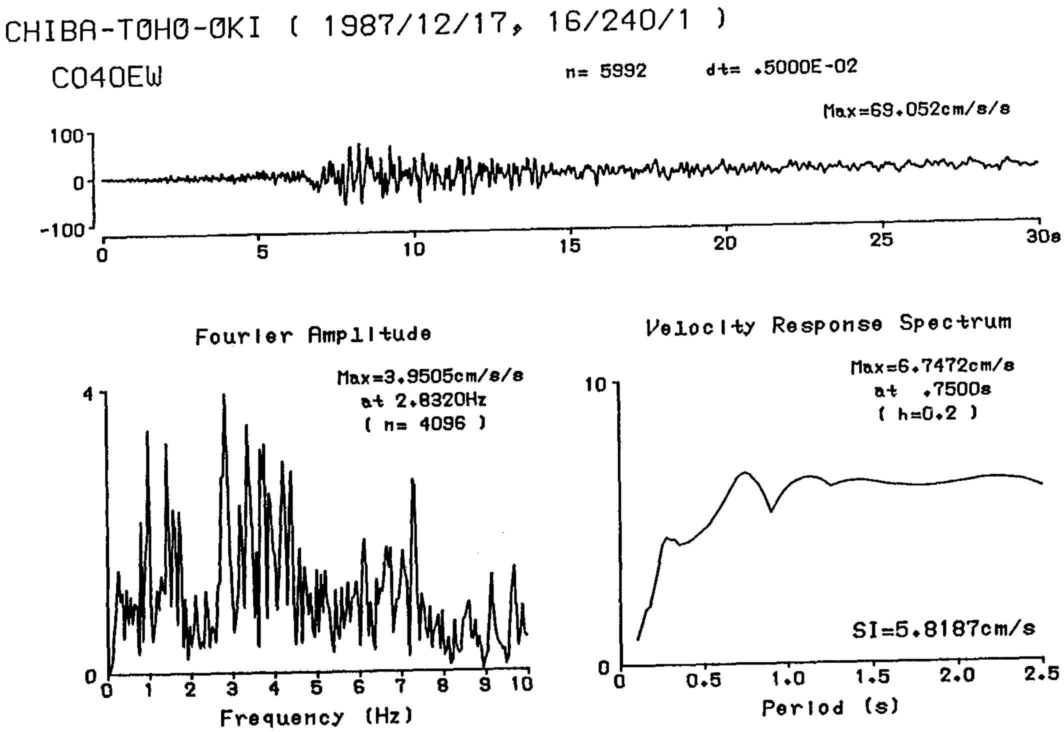

Fig.9(e) Ground Motion at GL-40 in Borehole CO

CHIBA-TOHO-OKI (1987/12/17, 16/240/1)

C101NS n= 5992 dt= .5000E-02

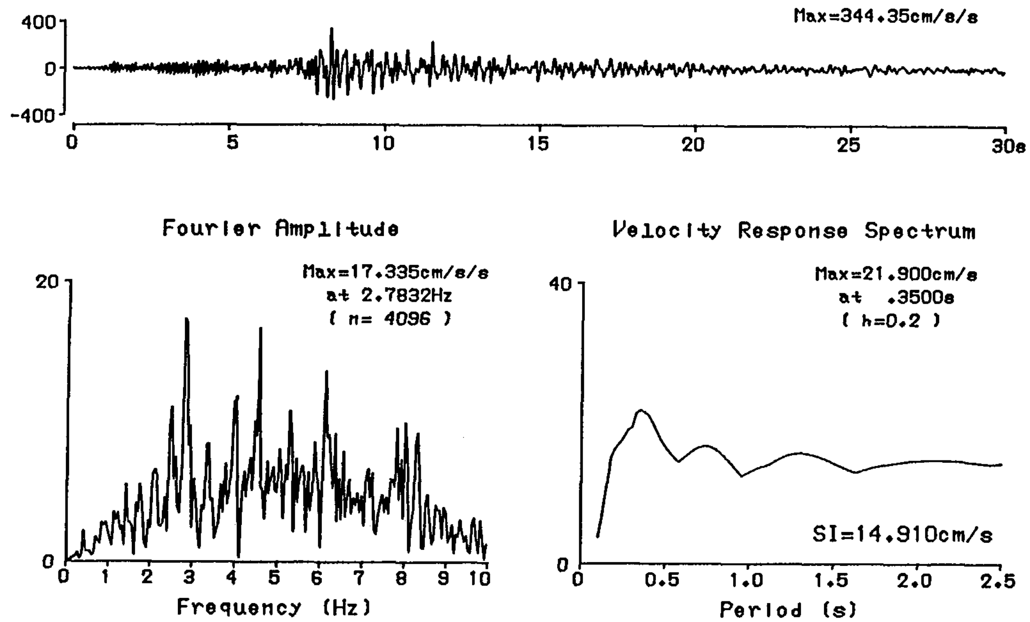

CHIBA-TOHO-OKI (1987/12/17, 16/240/1)

C101EW n= 5992 dt= .5000E-02

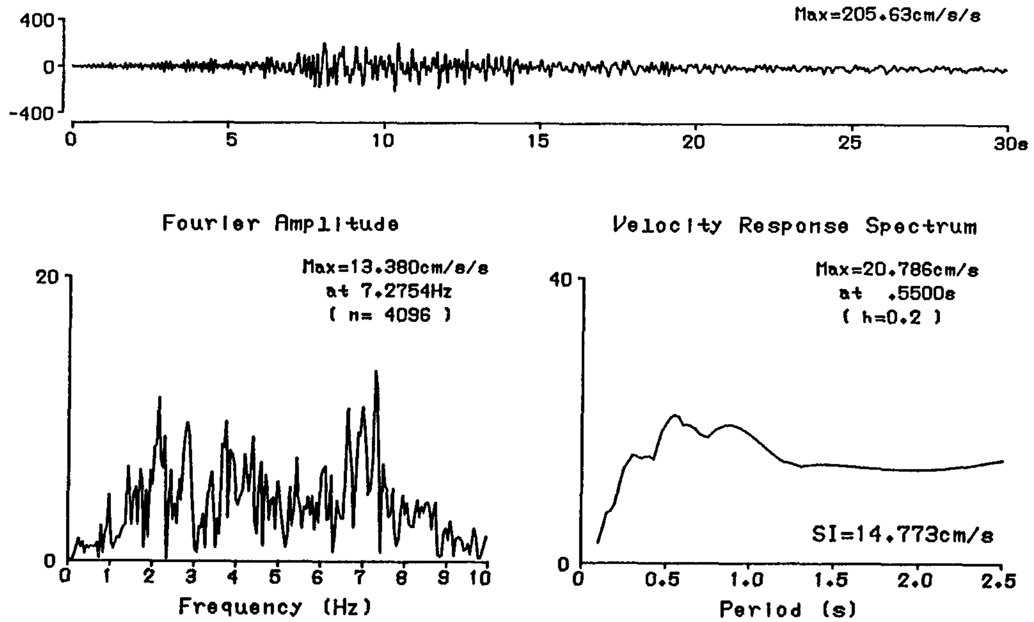

Fig.10(a) Ground Motion at GL-1 in Borehole C1

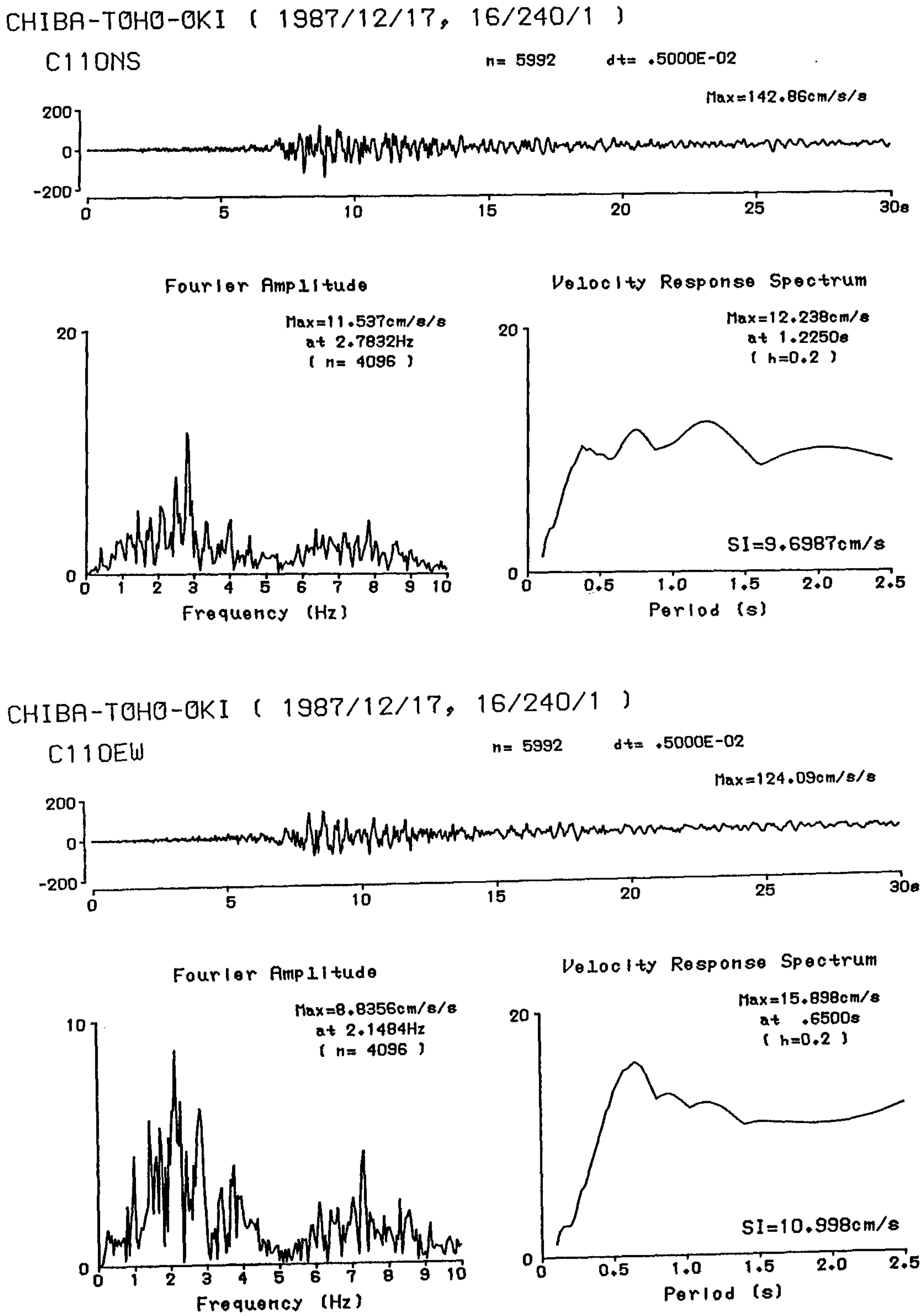

Fig.10(b) Ground Motion at GL-10 in Borehole C1

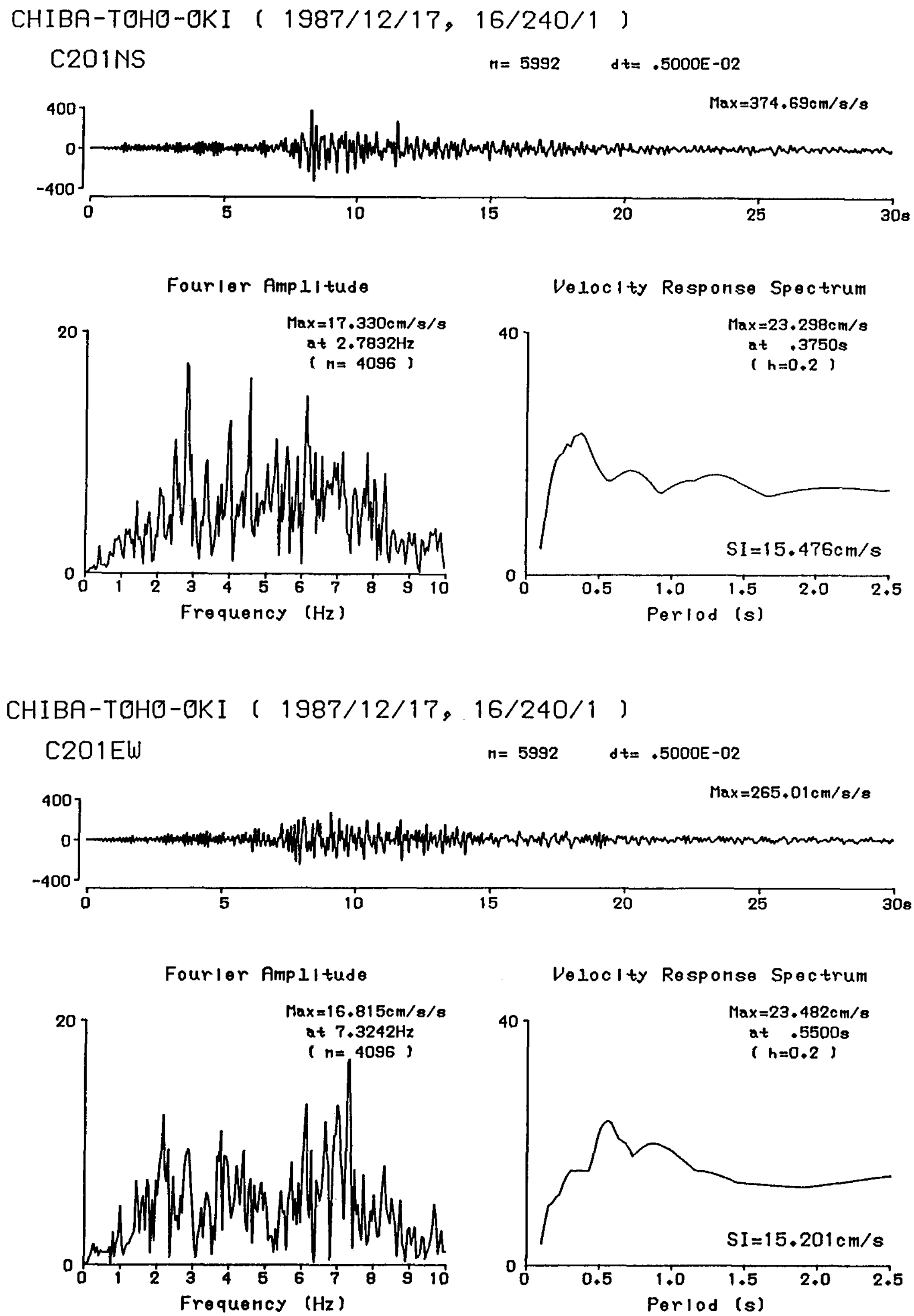

Fig.11(a) Ground Motion at GL-1 in Borehole C2

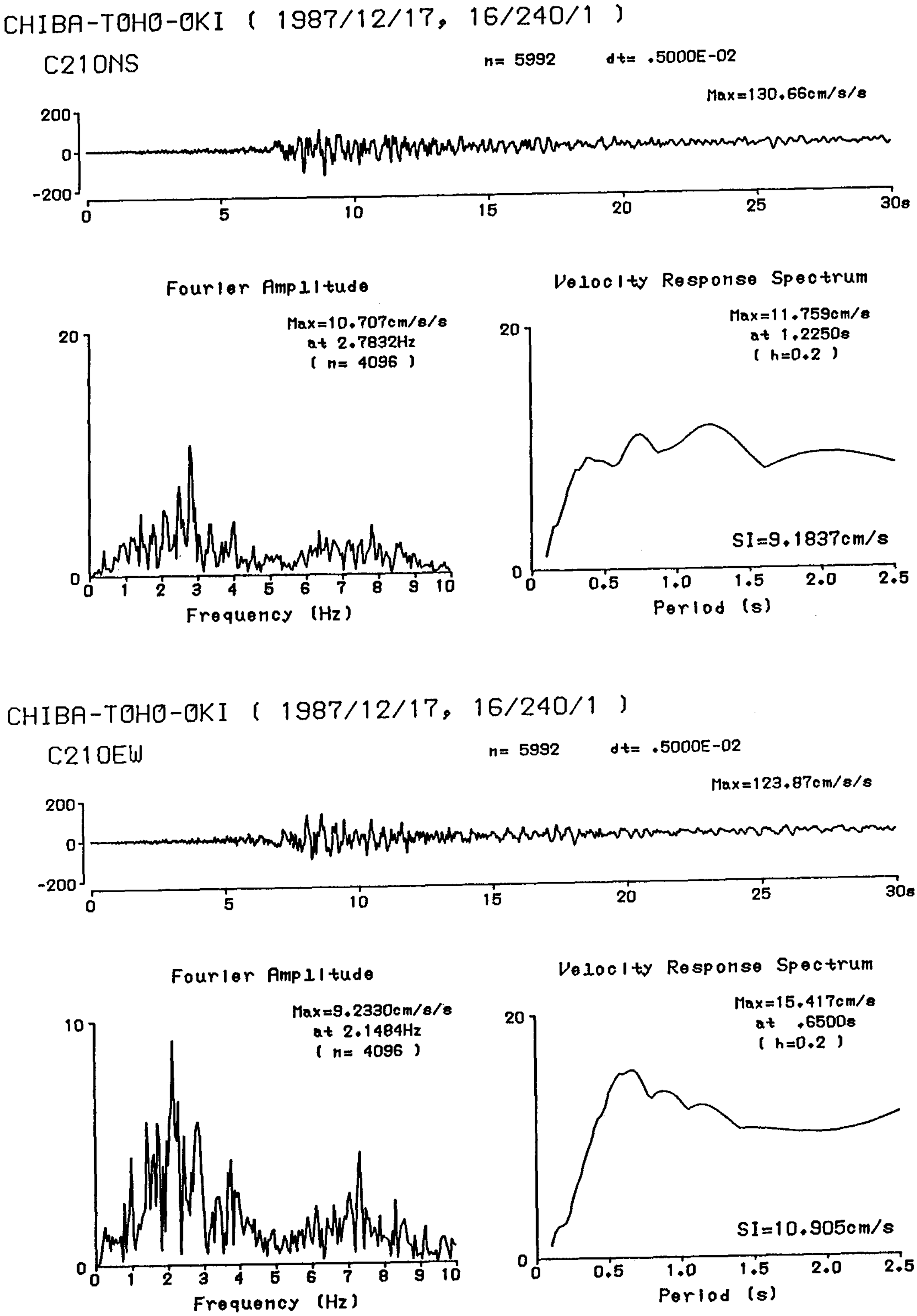

Fig.11(b) Ground Motion at GL-10 in Borehole C2

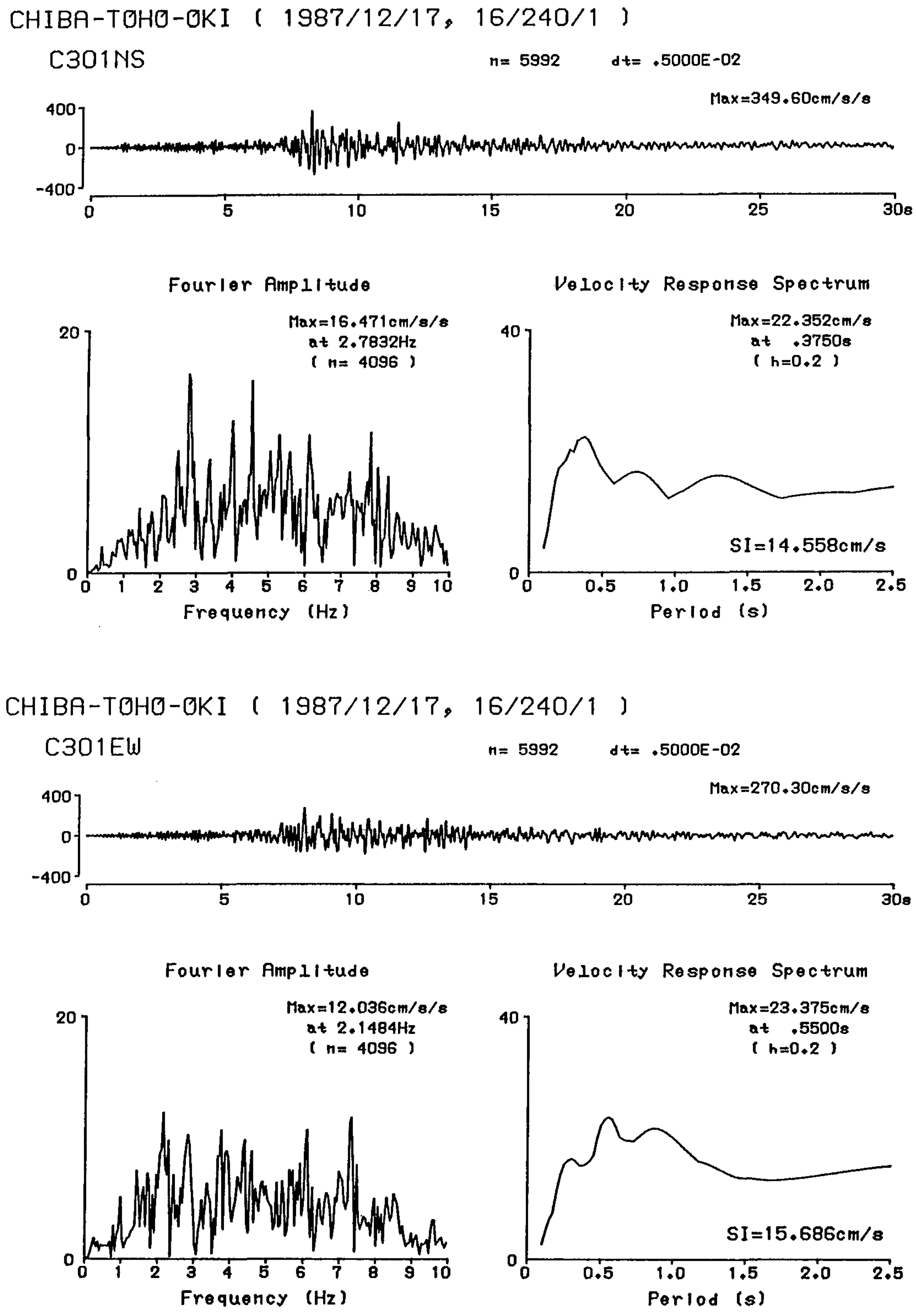

Fig.12(a) Ground Motion at GL-1 in Borehole C3

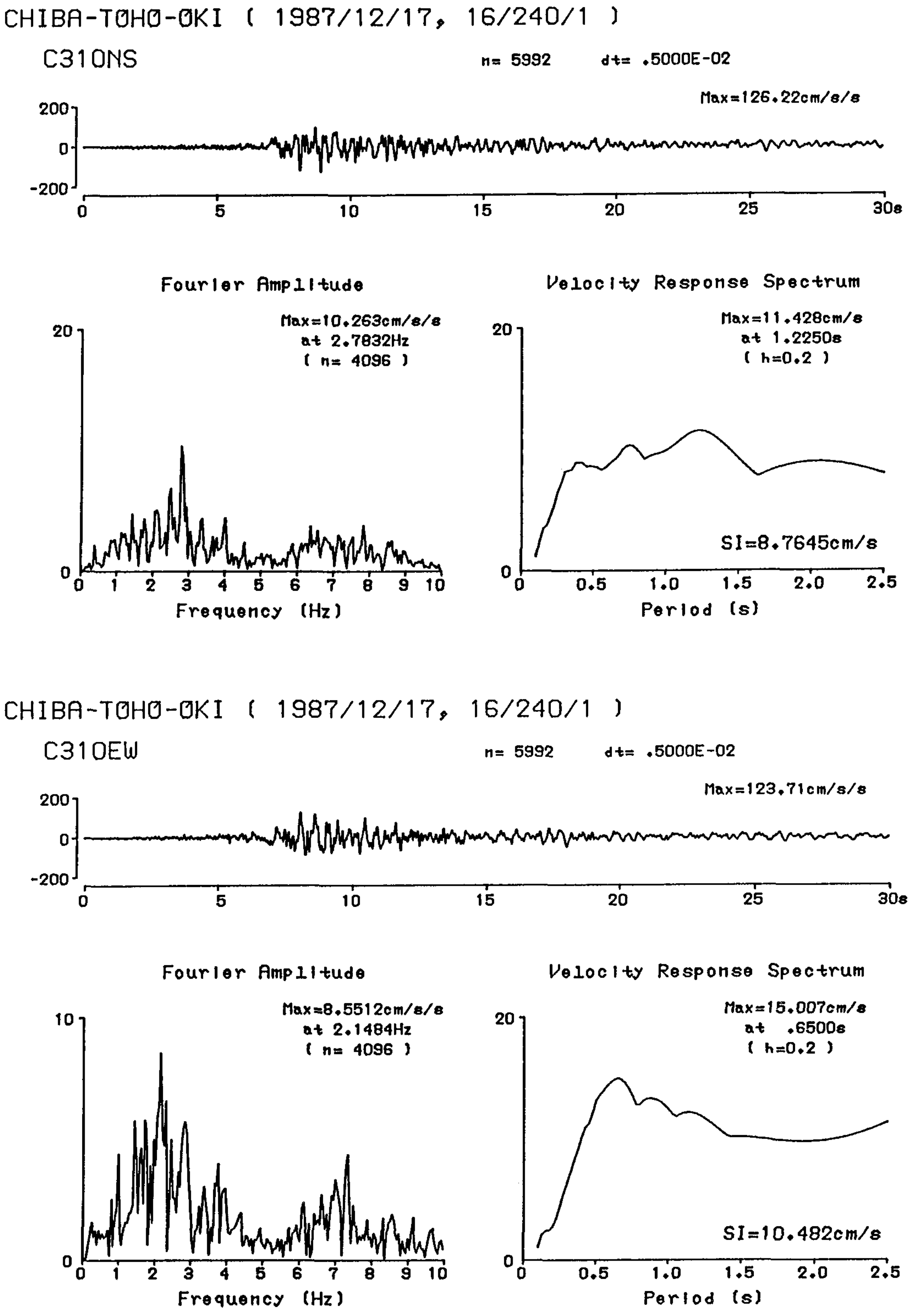

Fig.12(b) Ground Motion at GL-10 in Borehole C3

CHIBA-TOHO-OKI (1987/12/17, 16/240/1)

C401NS n= 5992 dt= .5000E-02

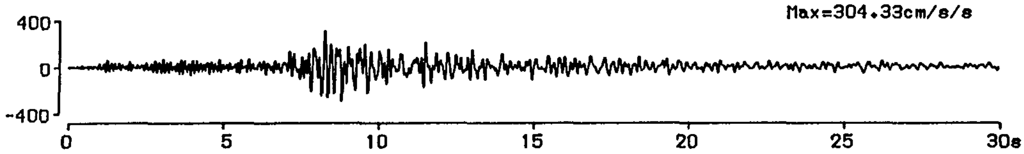

Fourier Amplitude

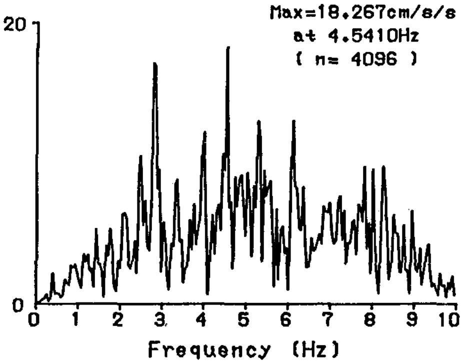

Velocity Response Spectrum

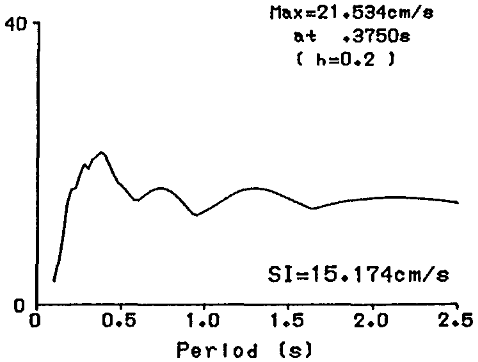

CHIBA-TOHO-OKI (1987/12/17, 16/240/1)

C401EW n= 5992 dt= .5000E-02

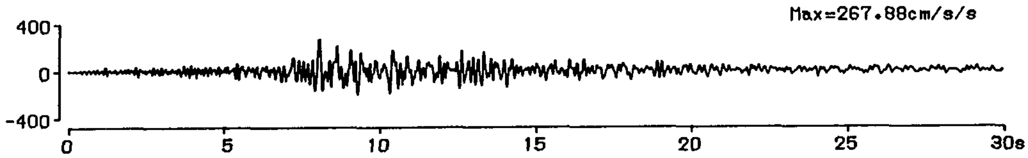

Fourier Amplitude

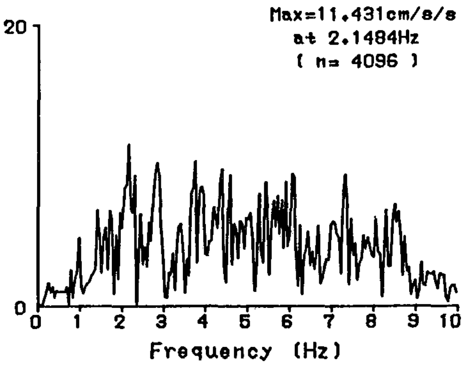

Velocity Response Spectrum

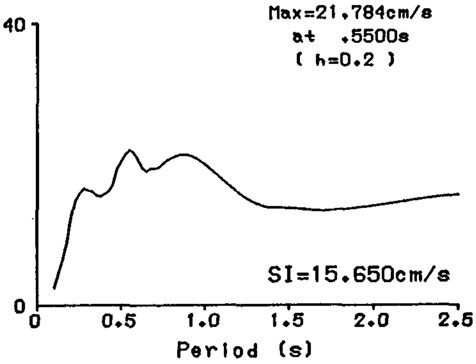

Fig.13(a) Ground Motion at GL-1 in Borehole C4

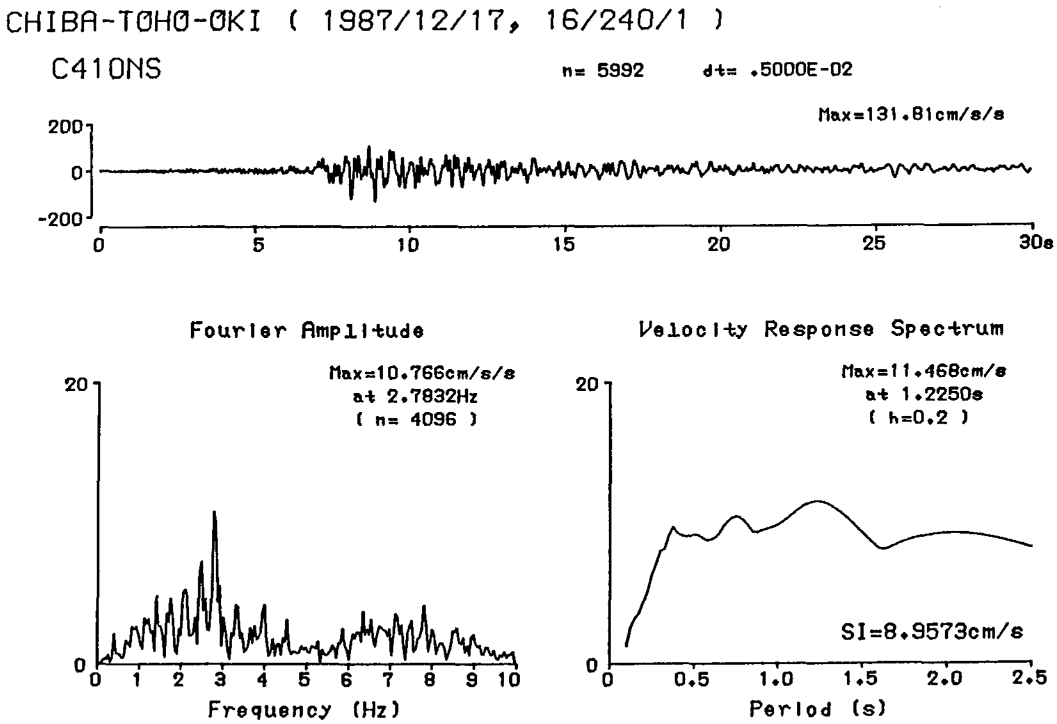

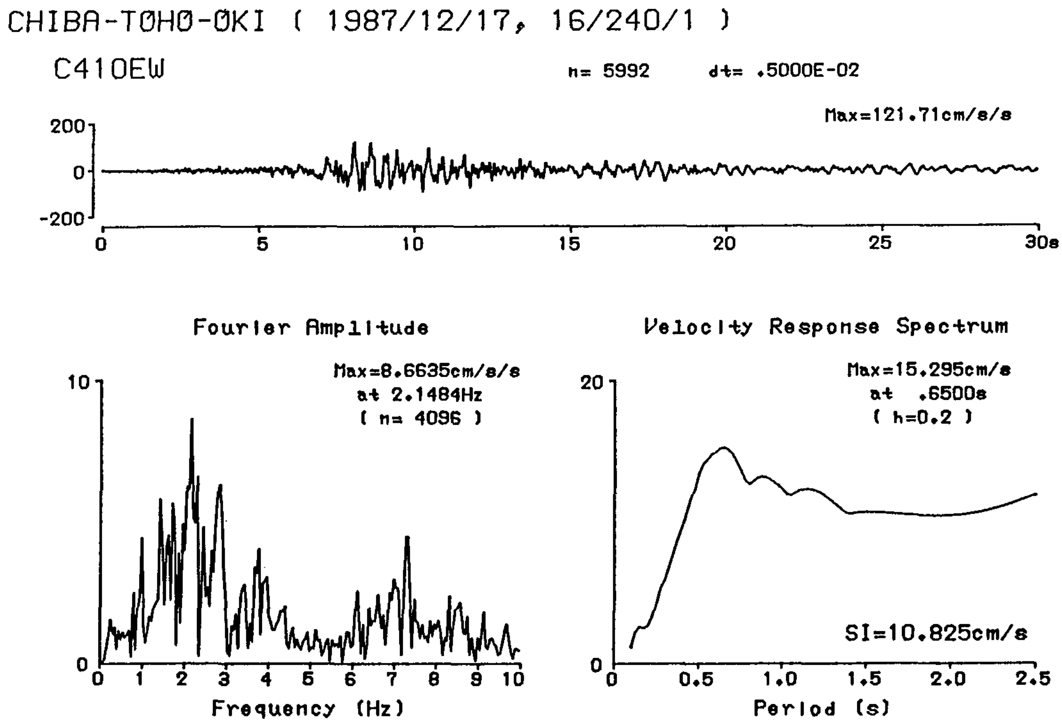

Fig.13(b) Ground Motion at GL-10 in Borehole C4

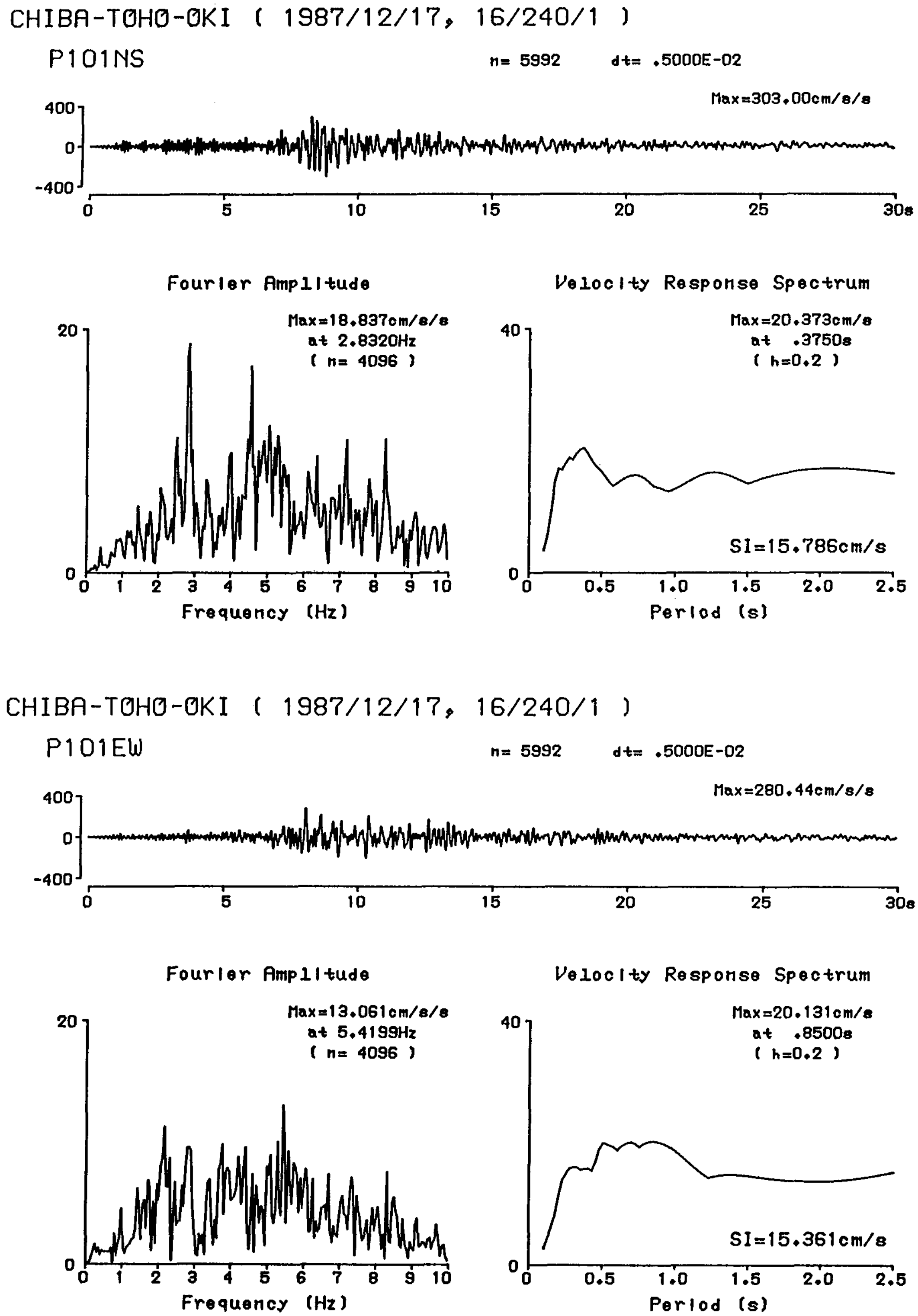

Fig.14(a) Ground Motion at GL-1 in Borehole P1

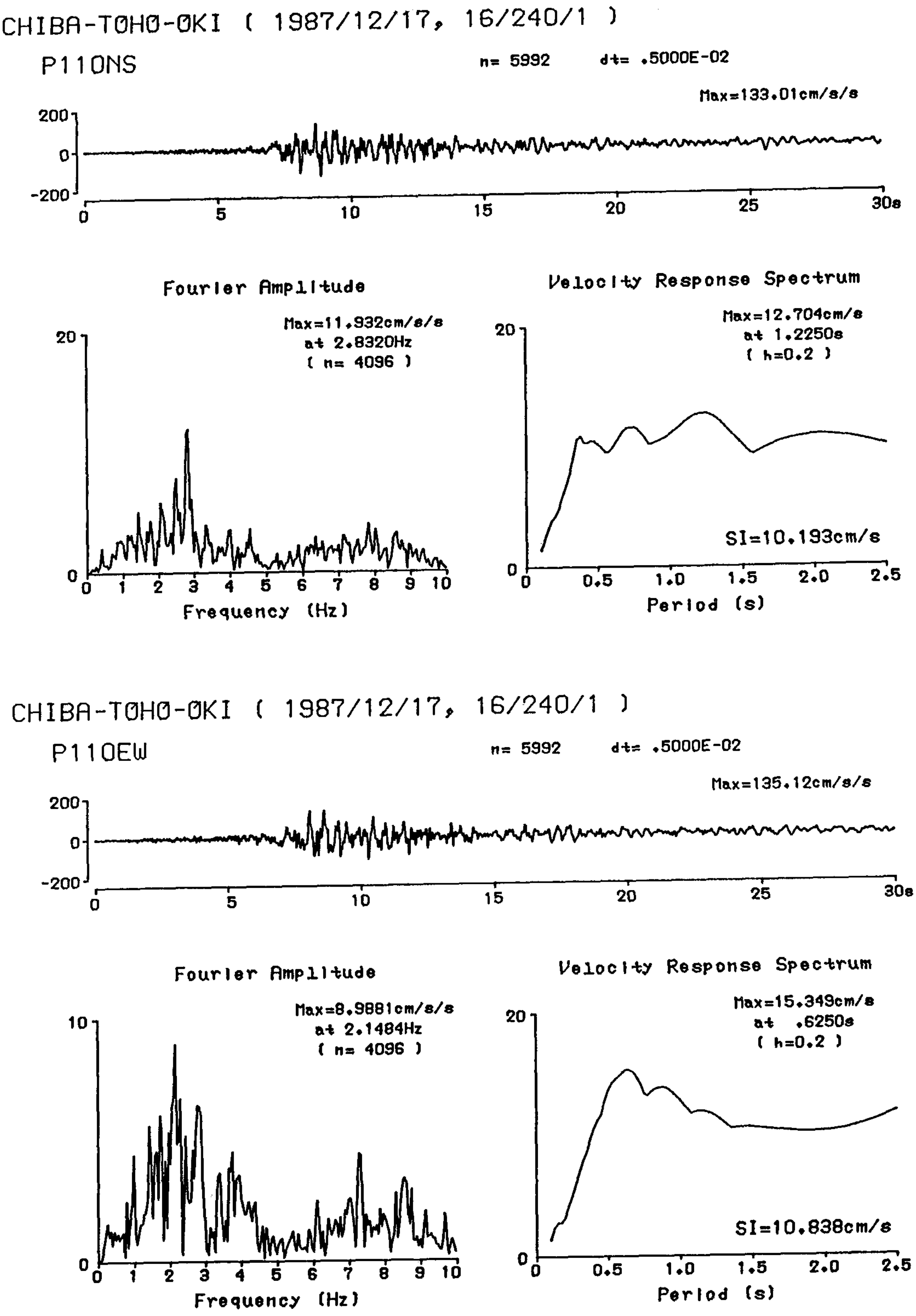

Fig.14(b) Ground Motion at GL-10 in Borehole P1

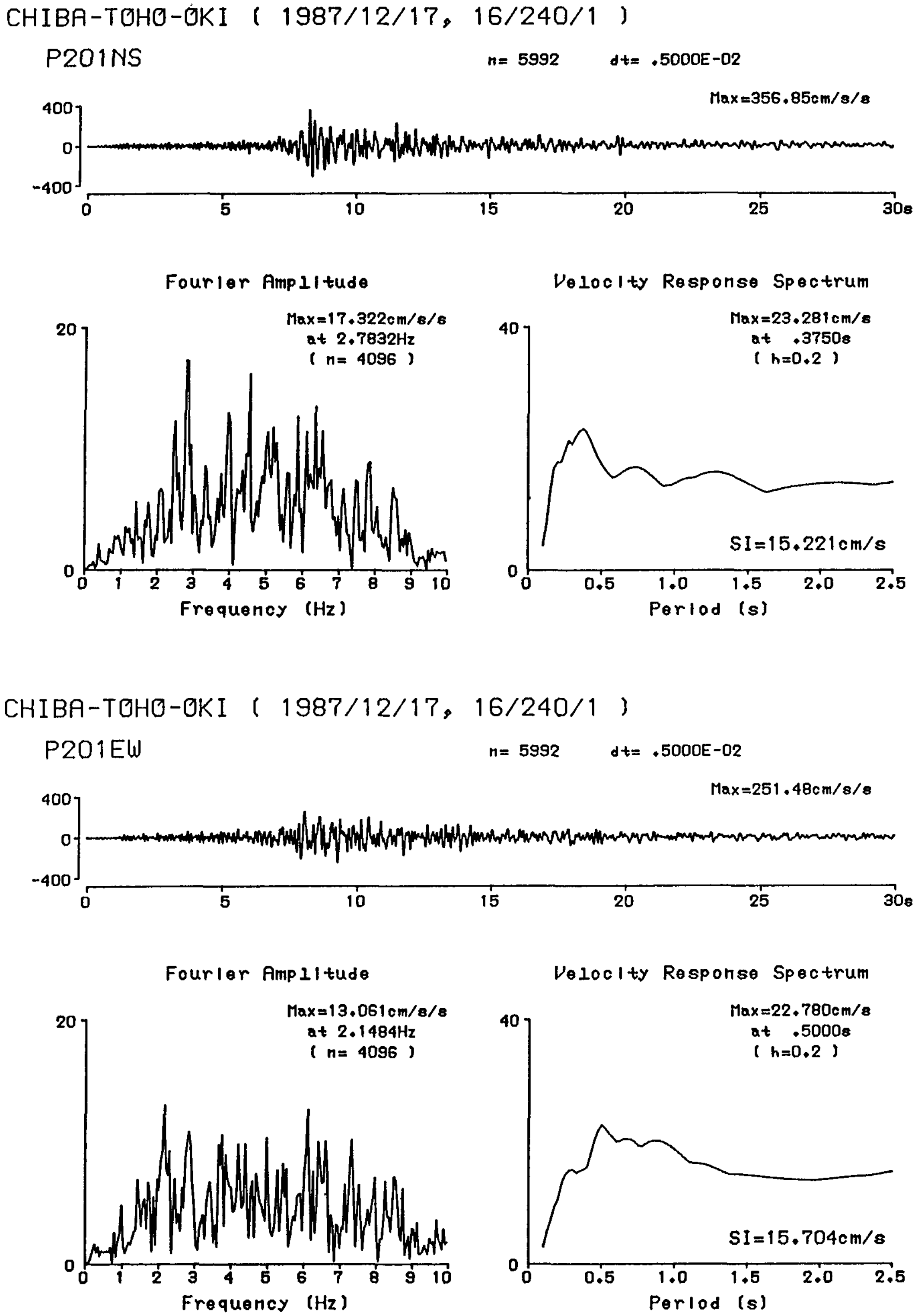

Fig.15(a) Ground Motion at GL-1 in Borehole P2

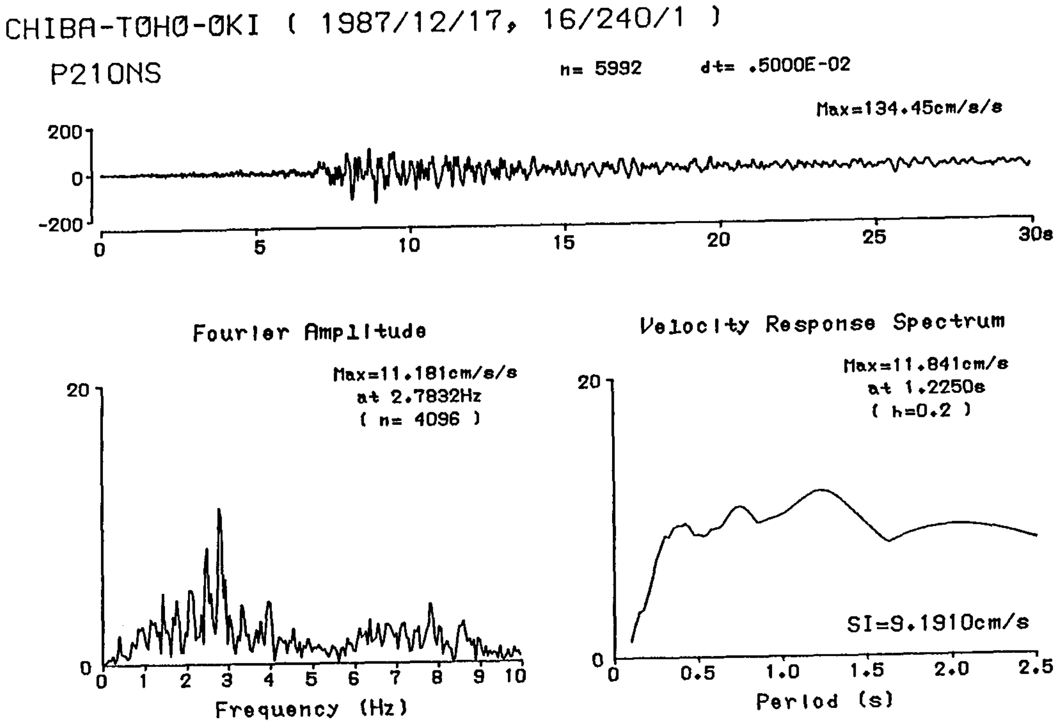

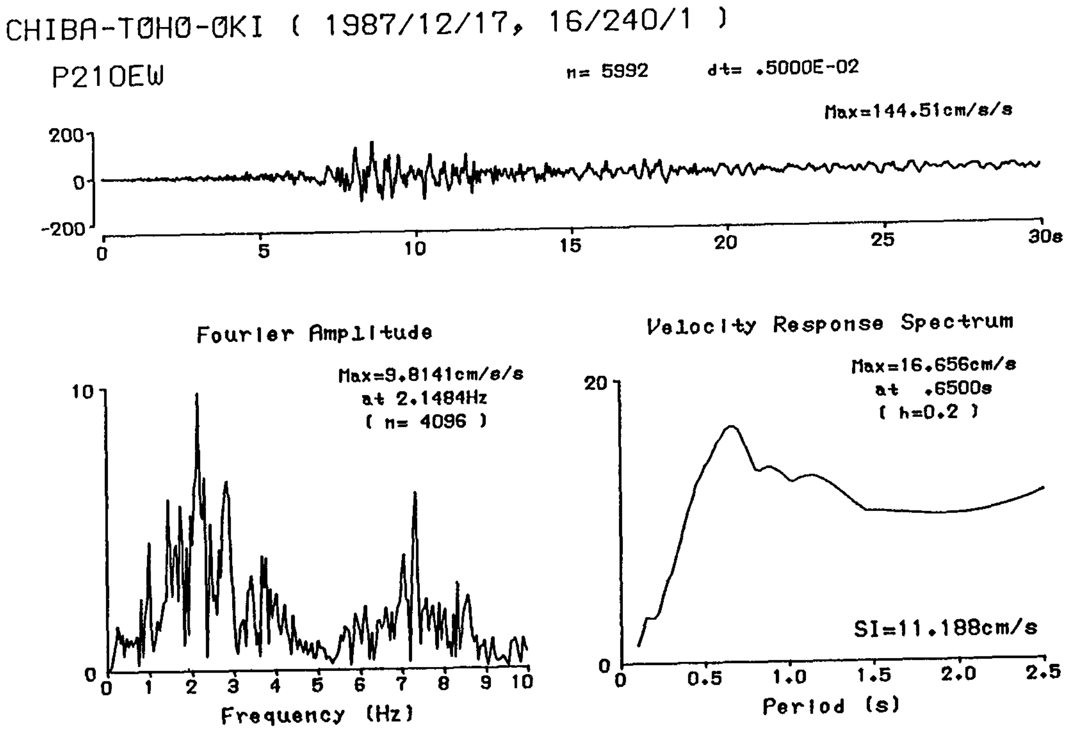

Fig.15(b) Ground Motion at GL-10 in Borehole P2

CHIBA-TOHO-OKI (1987/12/17, 16/240/1)

P301NS

n= 5992 dt= .5000E-02

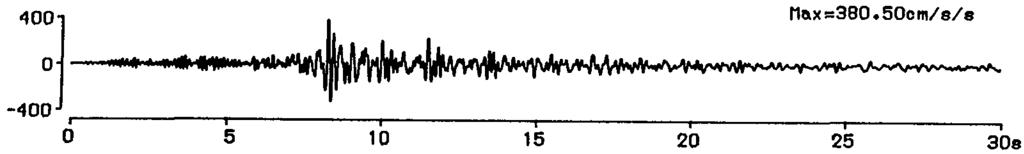

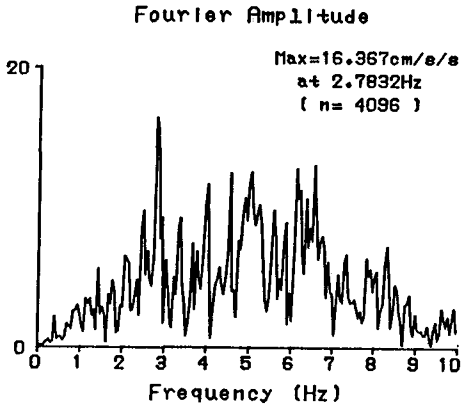

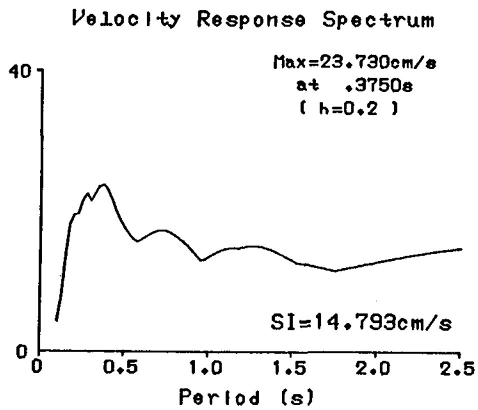

CHIBA-TOHO-OKI (1987/12/17, 16/240/1)

P301EW

n= 5992 dt= .5000E-02

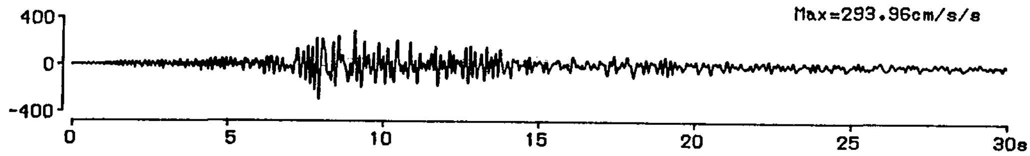

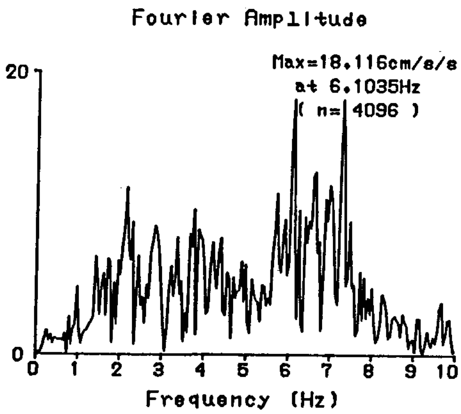

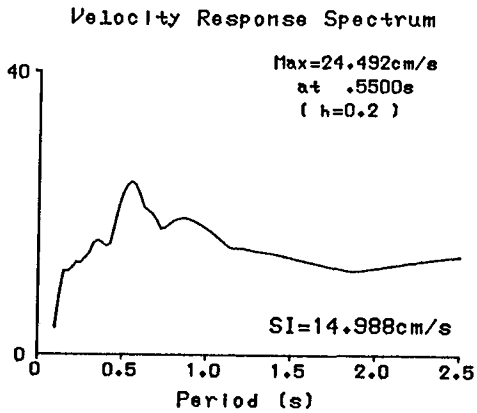

Fig.16(a) Ground Motion at GL-1 in Borehole P3

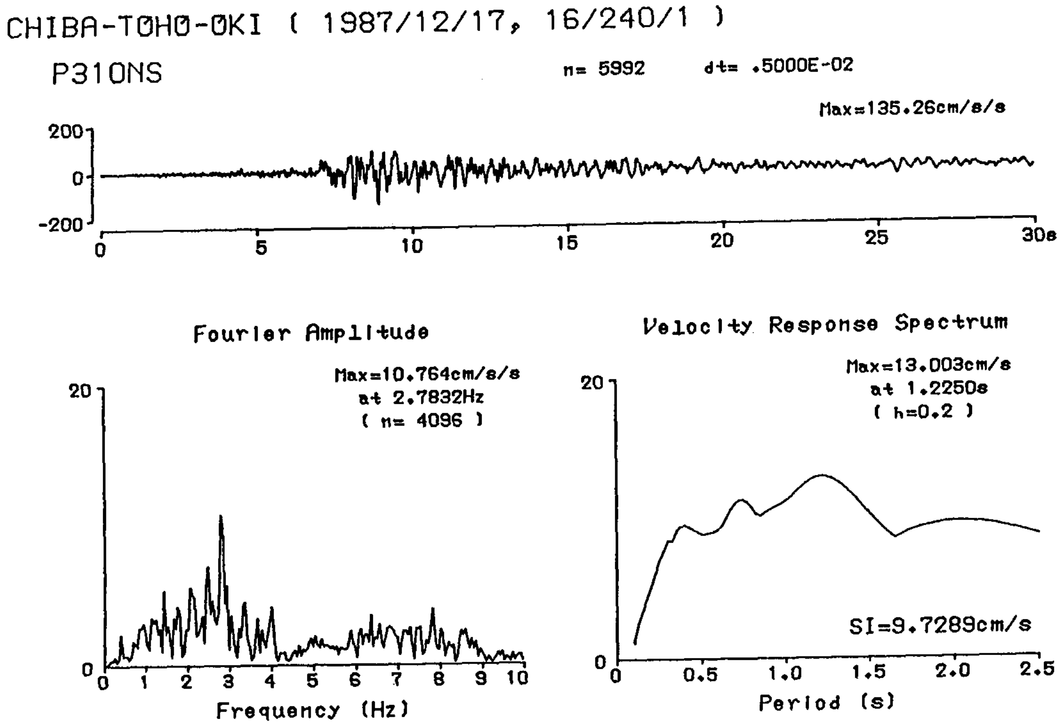

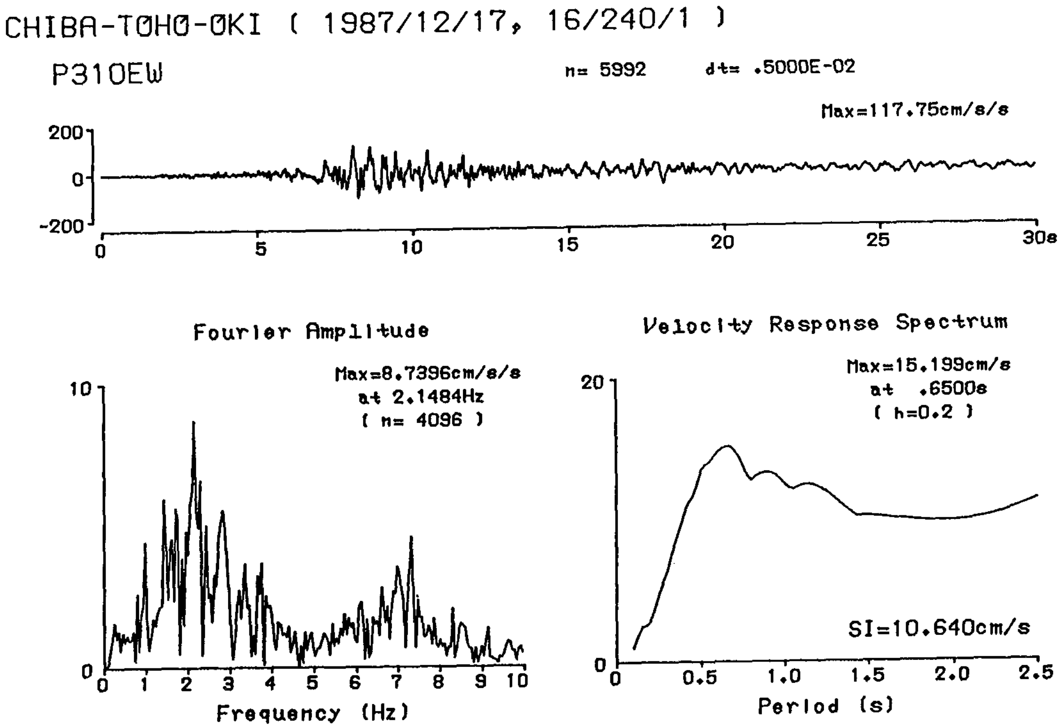

Fig.16(b) Ground Motion at GL-10 in Borehole P3

CHIBA-TOHO-OKI (1987/12/17, 16/240/1)

P401NS

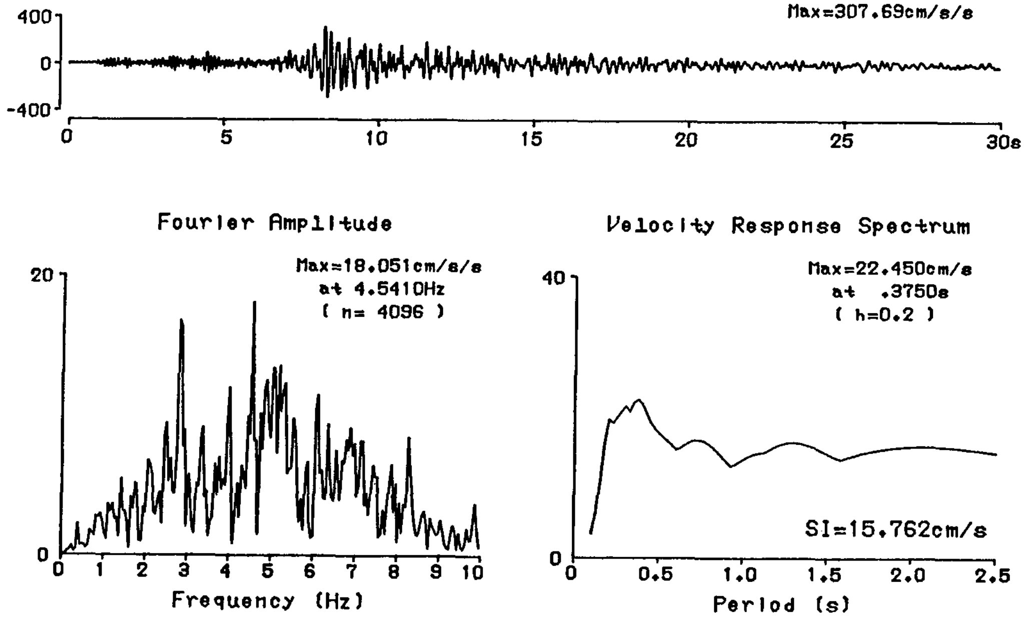

CHIBA-TOHO-OKI (1987/12/17, 16/240/1)

P401EW

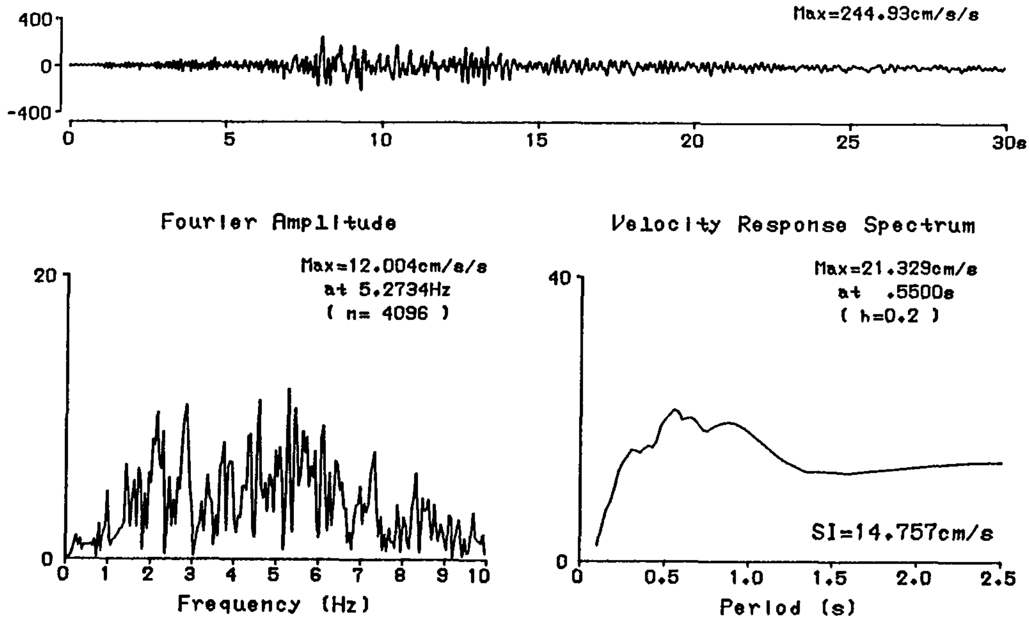

Fig.17(a) Ground Motion at GL-1 in Borehole P4

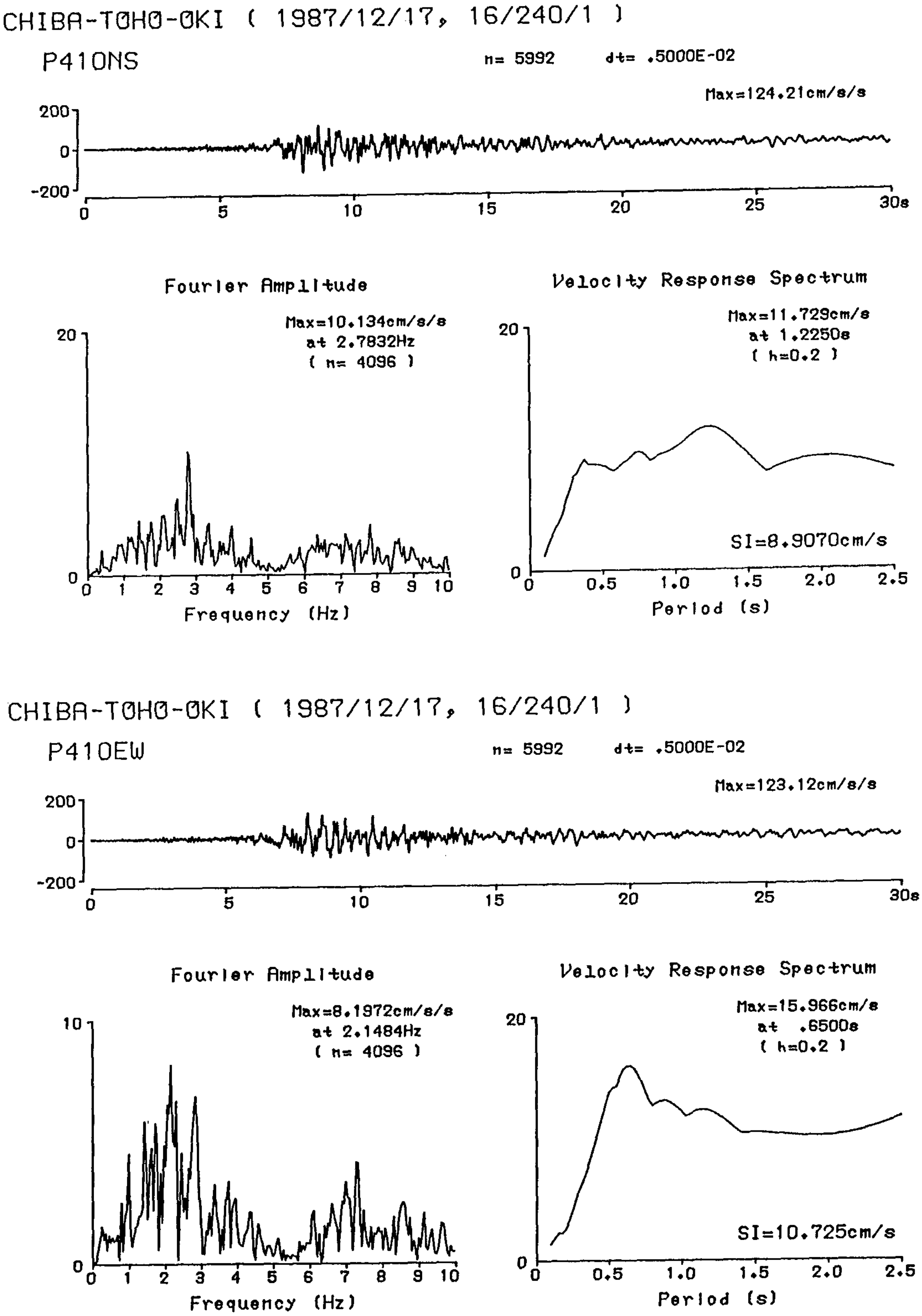

Fig.17(b) Ground Motion at GL-10 in Borehole P4

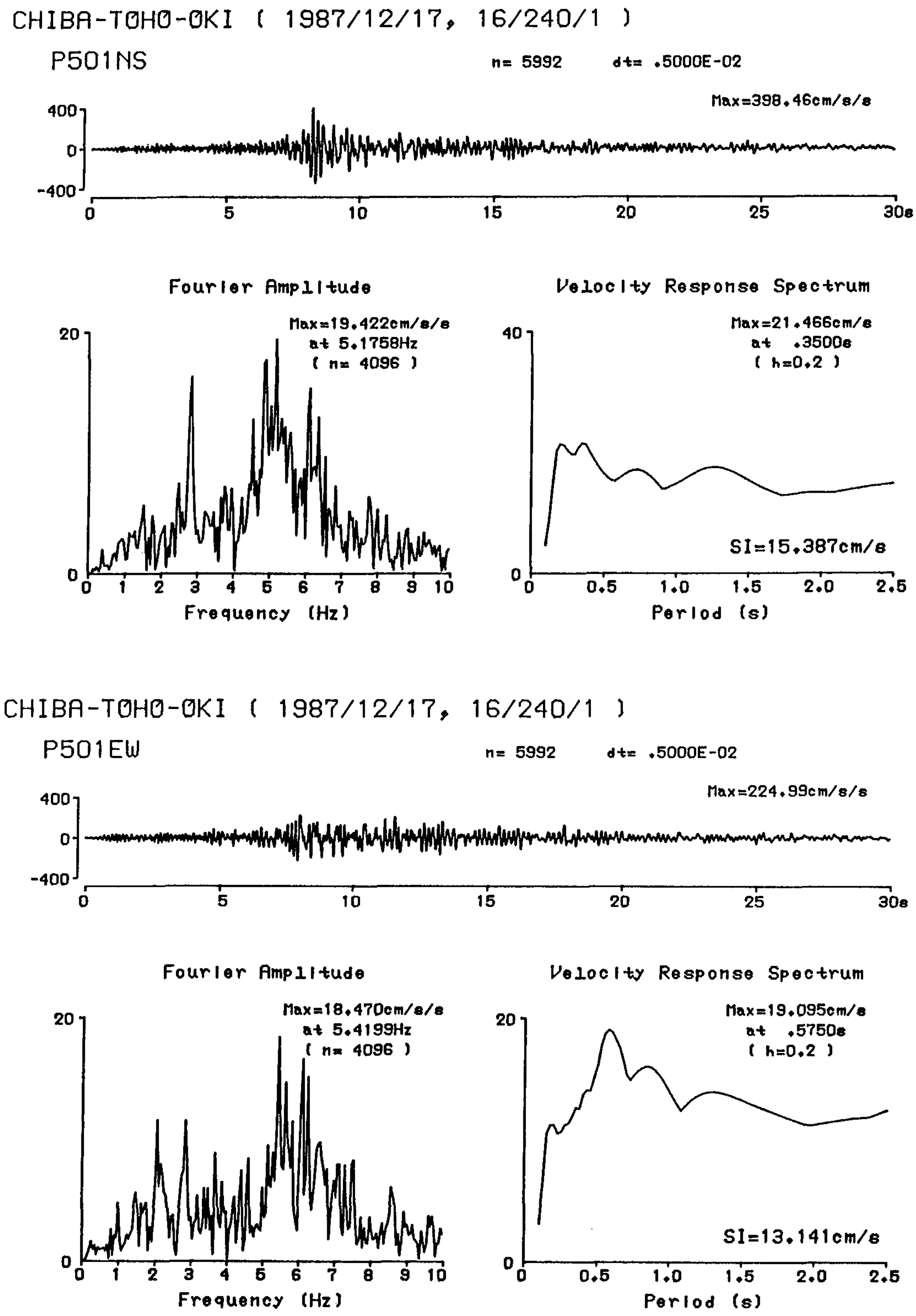

Fig.18(a) Ground Motion at GL-1 in Borehole P5

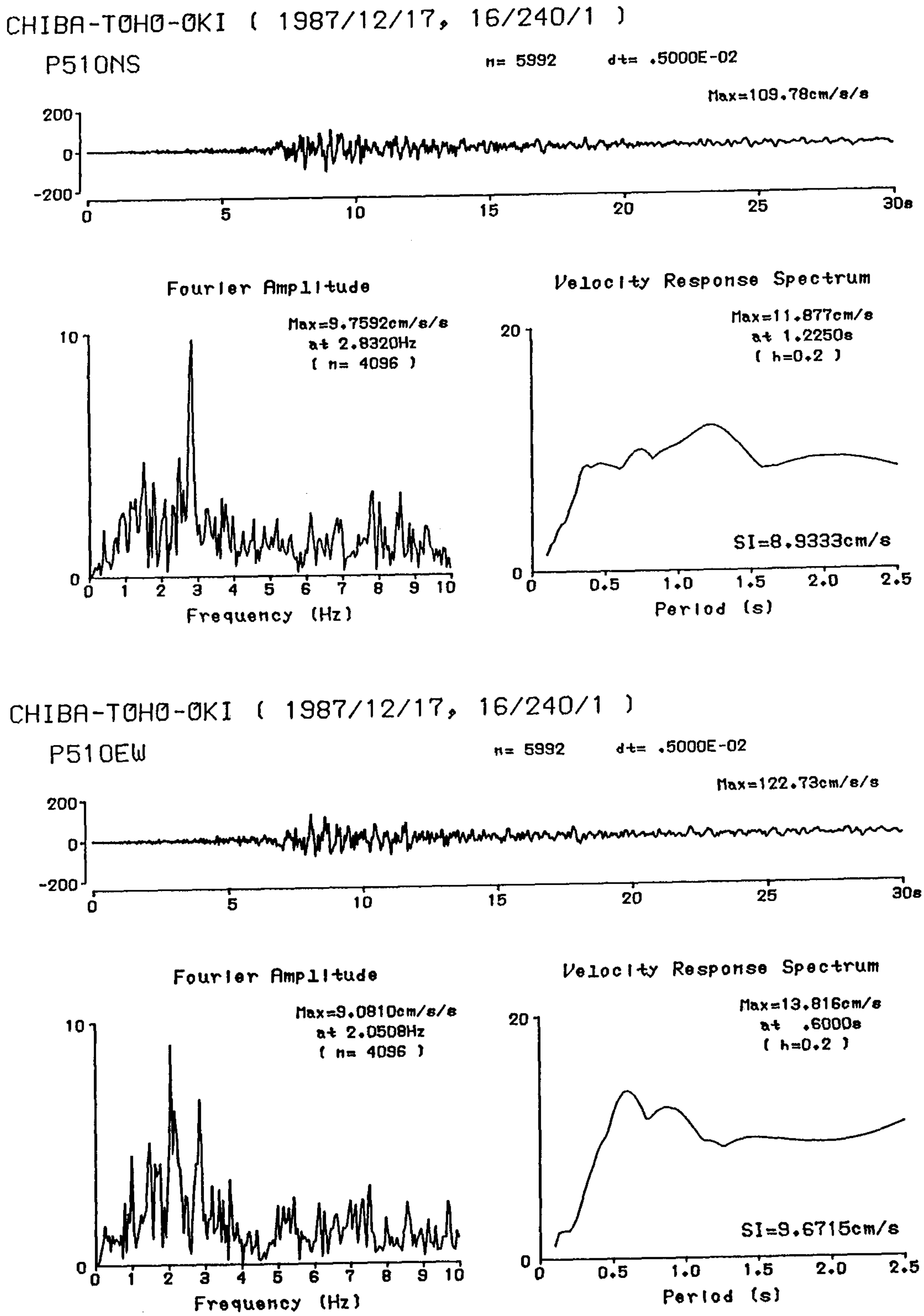

Fig.18(b) Ground Motion at GL-10 in Borehole P5

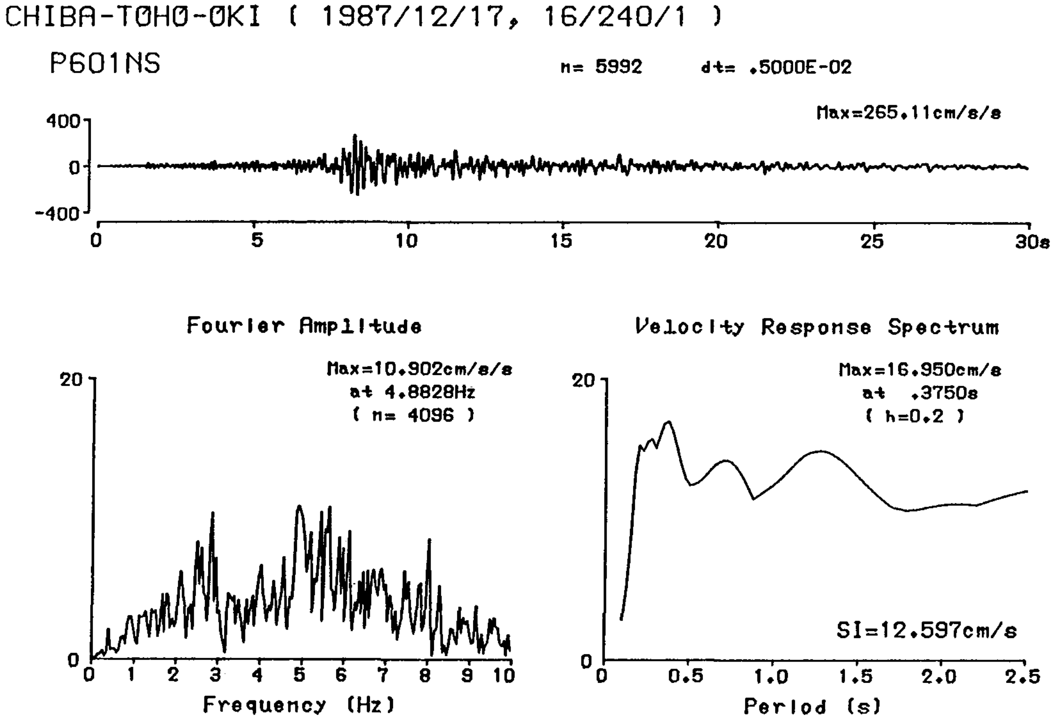

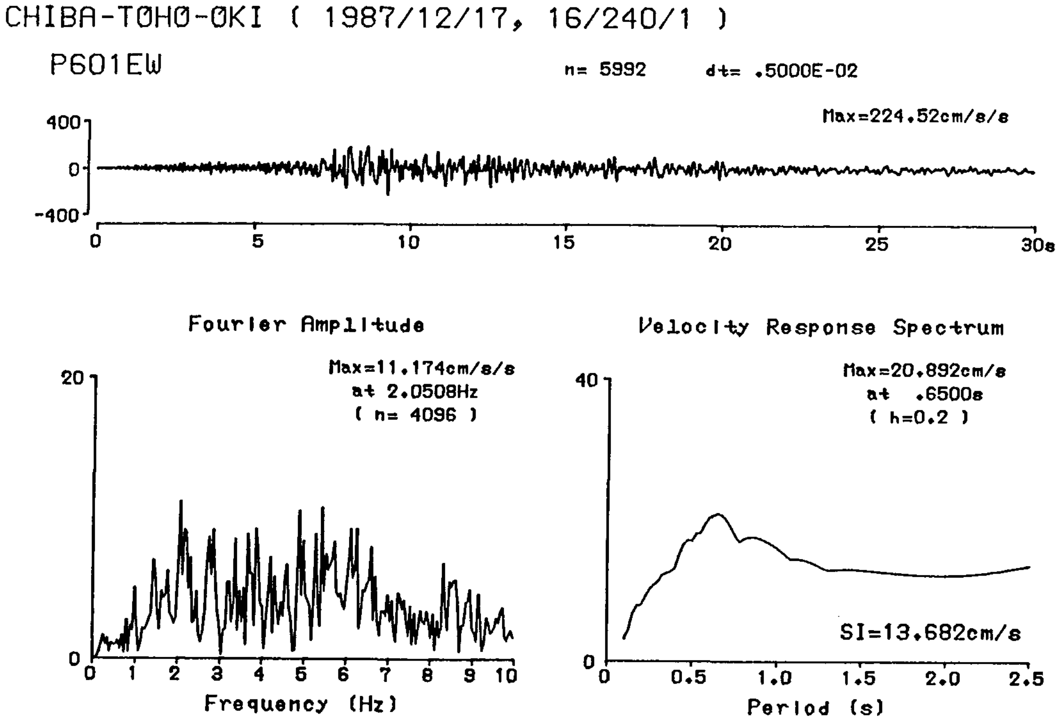

Fig.19(a) Ground Motion at GL-1 in Borehole P6

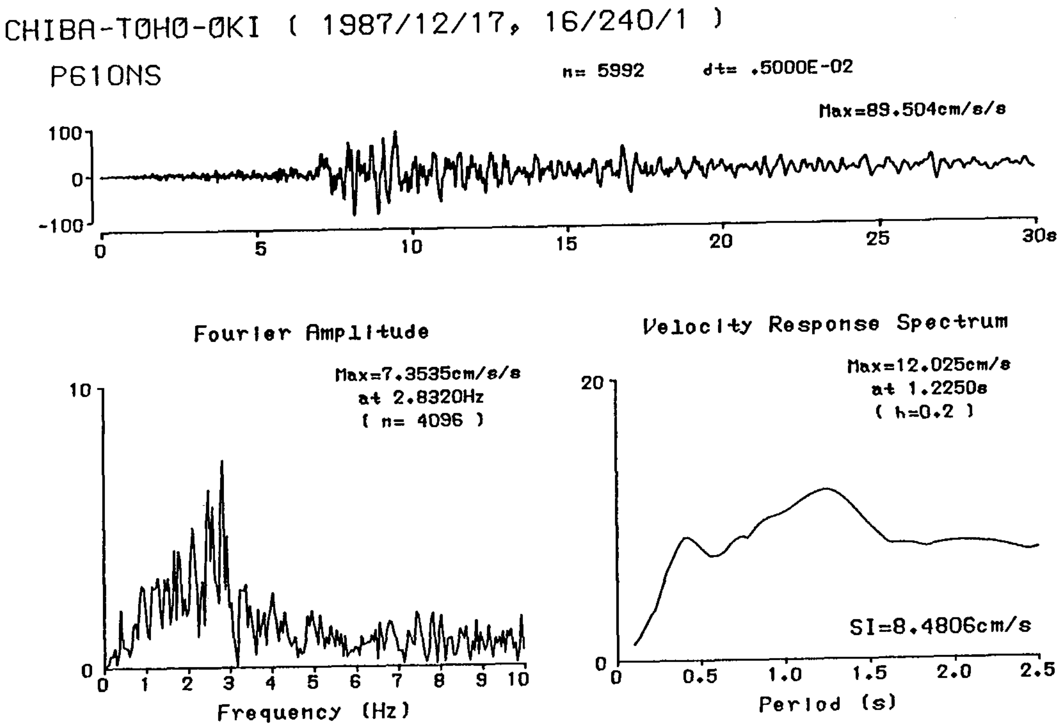

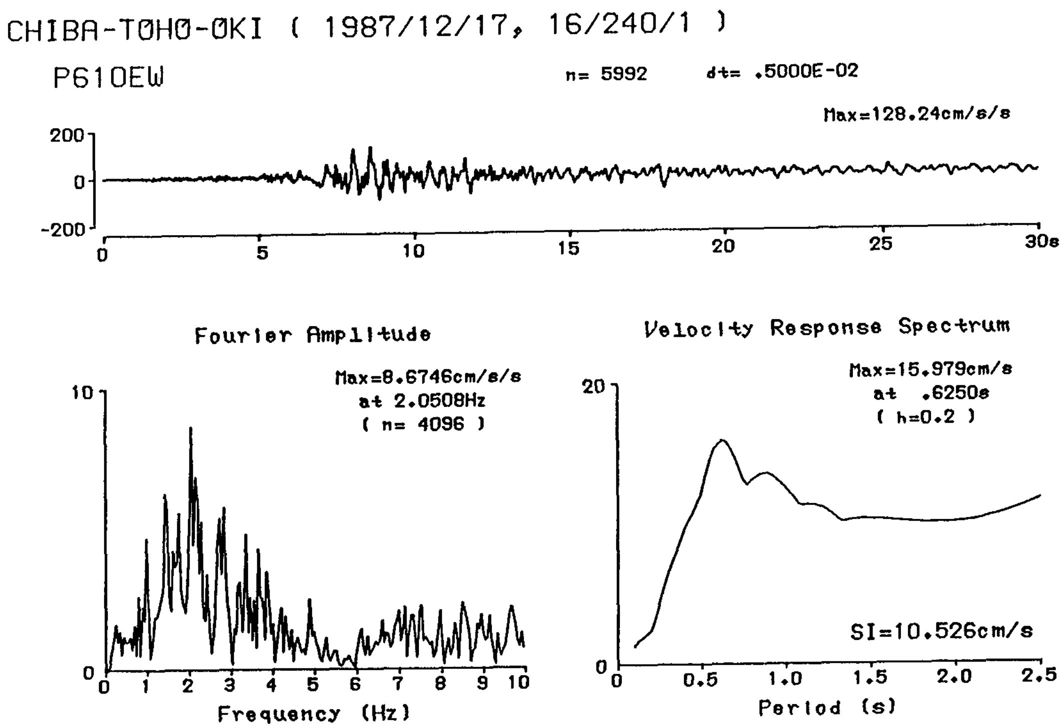

Fig.19(b) Ground Motion at GL-10 in Borehole P6